AD NUMBER

AD810327

LIMITATION CHANGES

TO:

Approved for public release; distribution is unlimited.

FROM:

**Distribution authorized to U.S. Gov't. agencies and their contractors;
Administrative/Operational Use; AUG 1966. Other requests shall be referred to Office of Naval Research, 875 North Randolph Street, Arlington, VA 22203-1995.**

AUTHORITY

ONR notice, 27 Jul 1971

TECHNICAL REPORT 233-10

ON MODELING CAVITATION DAMAGE

By

A. Thiruvengadam

August 1966

HYDRONAUTICS, incorporated
research in hydrodynamics

Research, consulting, and advanced engineering in the fields of NAVAL and INDUSTRIAL HYDRODYNAMICS. Offices and Laboratory in the Washington, D. C., area: Pindell School Road, Howard County, Laurel, Md.

Citation Format: Full Citation (1F)

Accession Number:
AD0810327
Citation Status:
Active
Citation Classification:
Unclassified
Fields and Groups:
200400 - Fluid Mechanics
Corporate Author:
HYDRONAUTICS INC LAUREL MD
Unclassified Title:
(U) ON MODELING CAVITATION DAMAGE.
Title Classification:
Unclassified
Descriptive Note:
Technical rept.,
Personal Author(s):
Thiruvengadam, A
Report Date:
Aug 1966
Media Count:
57 Page(s)
Cost:
$9.60
Contract Number:
Nonr-3755(00)
Report Number(s):
TR-233-10
Project Number:
NR-062-293
Report Classification:
Unclassified

Distribution Change Order Refer to Change Authority

Descriptors:

(U) *DAMAGE, *CAVITATION, MODEL TESTS, MATHEMATICAL MODELS, BUBBLES, PRESSURE, DAMPING, COMPRESSIVE PROPERTIES, VIBRATION, HYDRODYNAMICS, LIQUIDS, GASES, VAPORS

Identifier Classification:

Unclassified

Abstract:

(U) The intensity of bubble collapse is defined as the power transmitted per unit surface area of the bubble when the collapse pressure is a maximum and is given by the square of the collapse pressure divided by the acoustic impedence of the liquid. The efficiency of damage is defined as the ratio of the intensity of erosion of the material to the intensity of bubble collapse. Quantitative analysis is made to show how this efficiency would be affected by various physical effects such as inertia, damping of gas and vapor inside the bubble, heat transfer, compressibility, surface tension and viscosity. Experimental results with vibratory apparatus show that the efficiency of damage is primarily controlled by the damping of non-condensible gases and vapor. At higher temperature viscosity also seems to be important. Within the range of experiments, surface tension of the liquids tested seems to be unimportant. The group of non-dimensional numbers derived from the above analysis as used to formulate a modeling technique to predict the rate of depth of erosion in actual operating hydrodynamic systems. (Author)

Abstract Classification:

Unclassified

Distribution Limitation(s):

01 - APPROVED FOR PUBLIC RELEASE

Source Code:

174500

Document Location:

DTIC AND NTIS

Change Authority:

ST-A ONR NOTICE, 27 JUL 71

HYDRONAUTICS, Incorporated

TECHNICAL REPORT 233-10

ON MODELING CAVITATION DAMAGE

By

A. Thiruvengadam

August 1966

Prepared Under

Office of Naval Research
Department of the Navy
Contract No. Nonr-3755(00) (FBM)
NR 062-293

TABLE OF CONTENTS

LIST OF FIGURES

NOTATION

I_a	Acoustic intensity
I_c	Intensity of collapse
I_d	Intensity of damage
p_c	Bubble collapse pressure
ρ_ℓ	Density of liquid
C_ℓ	Sound speed in liquid
C_m	Sound speed in liquid-vapor bubble mixture
P_o	Reference pressure at infinity
R_m	Maximum radius of bubble
R_f	Final collapse radius of bubble
Q_o	Partial pressure of gas inside the bubble at the beginning of collapse
k	Ratio of specific heats for the permanent gas inside the bubble
S_ℓ	Specific heat per unit mass of liquid
S_g	Specific heat per unit mass of gas
$\Lambda_\ell = (Dt_c)^{\frac{1}{2}}$	Thermal diffusion layer in the liquid
D	Thermal diffusivity
t_c	Time of collapse
ρ_g	Density of gas
γ	Surface tension of the liquid

R_n	Radius of the nucleus of the bubble
p_v	Vapor pressure of the liquid
p_g	Partial pressure of gas inside the nucleus
N_i	Number of moles of the gas
θ	Perfect gas law constant
T_a	Ambient temperature
m_ℓ	Mass of liquid evaporated
ρ_v	Density of the vapor
m_g	Mass of gas inside the bubble
α_g	Mass concentration of the gas in liquid
Γ_g	Volume concentration of gas in liquid
M_v	Molecular weight of vapor
M_g	Molecular weight of gas
D_g	Diffusivity of gas in liquid
H	Heat of vaporization for the entire bubble
L	Latent heat of vaporization
ΔT	Temperature difference between the bubble and the liquid
T_B	Boiling point in the liquid
v	Velocity of liquid adjacent to the interface
v'	Velocity of the vapor adjacent to the interface
$U_B = R = \frac{dR}{dt}$	The velocity of the interface; i.e., bubble wall

M_w	Bubble wall Mach number
M_{w_1}	Mach number with respect to sound speed in gas
M_{w_2}	Mach number with respect to sound speed in liquid
C_g	Sound speed in gas
W_w	Weber number of the bubble motion
R_w	Reynolds number of the bubble motion
ν	Kinematic viscosity of the liquid
ξ_o	Amplitude of the specimen in the vibratory test
ω_o	Frequency of the specimen
U_o	Velocity of the specimen
μ	Frequency parameter
a	Radius of the specimen
λ	Wave length in liquid
V	Reference velocity in the free stream for flow experiments
M	Mach number of the flow
R_e	Reynolds number of the flow
σ	Cavitation parameter
β_ℓ	Coefficient of compressibility of liquid

SUMMARY

Similar to the definition of the intensity of cavitation damage, the intensity of cavitation bubble collapse is defined as the power transmitted per unit surface area of the bubble when the collapse pressure is a maximum. The intensity of collapse is given by the square of the maximum collapse pressure divided by the acoustic impedance ($\rho_\ell C_\ell$) of the liquid. Various physical effects such as inertial effects, damping due to non-condensible gases, thermal effects, compressibility effects, surface tension effects and viscous effects on the maximum collapse pressure are considered. The efficiency of damage given by the intensity of damage divided by the intensity of collapse is shown to depend principally on the dissolved gas content of the liquid (using the data obtained from the vibratory cavitation damage apparatus). It is also shown that the vapor itself might act as a damper near boiling point since the bubble wall temperatures increase rapidly at these temperatures. When the vapor pressure becomes important, viscosity also seems to affect the efficiency of damage as evidenced by the behavior of aniline. The efficiency of damage is independent of the surface tension of the liquid within the range of tests.

The above results from the vibratory experiments are used to propose a modeling technique to predict the rate of depth of erosion in actual operating hydrodynamic systems. One of the primary questions to be answered is the magnitude of the pressure field that drives the bubble to collapse. The dependence

of this pressure field on other hydrodynamic scaling parameters such as Reynolds number, Mach number and the cavitation parameter will decide the success of the proposed model technique.

INTRODUCTION

At the present state of knowledge it is possible to predict from model tests the various hydrodynamic forces such as drag, lift, thrust, etc. Similarly it would be highly desirable to predict the intensity of cavitation damage in prototypes by conducting model tests in the laboratory. As of now it is not possible to achieve this objective because there are no scaling laws that relate the model-prototype behavior. It is the purpose of this report to formulate such scaling laws and to discuss the physical phenomena that are scaled by these laws.

Figure 1 shows the flow behind a circular cylinder and the known and unknown parameters controlling cavitation damage. The geometrical and kinematic similarities of the overall cavity flow are controlled by the cavitation parameter and the Reynolds number. However the modeling of the phenomenon of cavitation damage requires that the energy of collapse of individual bubbles, the transmission of the energy to the material surface and the absorption of the energy by the material in its deformation and fracture be scaled also. Hence the problem is to define the above phases of energy transmission and absorption quantitatively and to determine the parameters that control the efficiency of this process, Figure 2. The intensity of material damage is defined in References 1 and 2 as

$$I_d = \frac{i\, S_e}{t} \qquad [1]$$

where

i is the depth of erosion,

t is the time of erosion, and

S_e is the erosion strength.

The erosion strength is defined as the energy absorbing capacity of the material per unit volume under the action of the erosive forces (3). If a similar definition for the intensity of bubble collapse can be derived, then the efficiency of this process would be given by

$$\eta = \frac{I_d}{I_c} \qquad [2]$$

where I_c is the intensity of bubble collapse. As of now, such a definition for the intensity of bubble collapse does not exist. One of the accomplishments of this report is such a definition which leads to logical scaling laws for the proposed technique of modeling cavitation damage.

INTENSITY OF BUBBLE COLLAPSE

It is assumed in this report that the collapse pressure emanating from an individual transient cavitation bubble causes the erosion. When a spherical bubble collapses with a bubble wall velocity U_B, the collapse pressure as derived by Rayleigh (4) is:

$$\frac{p_c^2}{\beta_\ell} = \rho_\ell U_B^2$$

where

p_c is the maximum collapse pressure,

β_ℓ is the coefficient of compressibility or bulk modulus of liquid,

ρ_ℓ is the density of liquid, and

U_B is the bubble wall velocity.

Hence

$$p_c = \rho_\ell C_\ell U_B \qquad [3]$$

since

$$\beta_\ell = \rho_\ell C_\ell^2$$

where C_ℓ is the sound speed in liquid.

The compressibility of the liquid β_ℓ would be greatly reduced due to the presence of cavitation bubbles. For this reason, the sound speed of the liquid-vapor bubble mixture, C_m, would be much less than C_ℓ. The actual sound speed used for computing the intensity of collapse should be C_m. However, very little is known about the values of C_m in cavitation clouds. Until more is known about C_m, the sound speed in liquid C_ℓ will be used for

computations. If we define the intensity of collapse as the radiated power per unit surface area of the bubble, then

$$\text{Intensity of collapse} = \frac{\text{Collapse power transmitted}}{\text{Surface area of bubble}}$$

$$I_c = \frac{p_c 4\pi R^2 \frac{dR}{dt}}{4\pi R^2}$$

$$= p_c U_B$$

since

$$U_B = \frac{dR}{dt} \quad .$$

Making use of Equation [3] we get

$$I_c = \frac{p_c^2}{\rho_\ell C_\ell} \quad . \qquad [4]$$

It is interesting to note that the intensity of bubble collapse is similar to the intensity of acoustic power radiated from a simple source (Figure 3). The dimensions of I_c are the same as I_d which are in power per unit area.

The above discussion shows that the intensity of collapse varies as the square of the maximum collapse pressure in a given liquid. Hence, it is important to consider the various physical effects that control this maximum collapse pressure.

THE MAXIMUM COLLAPSE PRESSURE

The maximum collapse pressure depends upon the shape of the bubble and the distance at which the bubble collapses. Furthermore, the growth and the collapse of the bubbles depend upon the following physical phenomena (5), (6):

A. Inertial effects
B. Damping effects
C. Thermal effects
D. Compressibility effects
E. Surface tension effects
F. Viscous effects.

In order to quantitatively evaluate the relative influence of these effects on the maximum collapse pressure, we will assume that the Besant-Rayleigh bubble collapse (5) causes the damage. (It is recognized that the Eisenberg bubble collapse (7), (8), may also be important. Hence, calculations for this case will be useful.)

A. Inertial Effects

Rayleigh (4) calculated the maximum collapse pressure for a spherical bubble collapsing in an infinite liquid; it is given by

$$p_c = \frac{P_o}{6.35}\left(\frac{R_m}{R_f}\right)^3 \qquad [5]$$

where

P_o is the pressure at infinity,

R_m is the maximum bubble radius at the start of collapse,

and R_f is the final bubble radius at the end of collapse .

This maximum collapse pressure occurs at a distance of 1.587 R_f from the center of collapse (4).

B. Damping Effects

Now the final radius to which the bubble collapses depends upon the amount of non-condensible gas present at the start of the collapse and on whether the gas is compressed isothermally or adiabatically. Assuming isothermal compression of the permanent gas inside the bubble, Rayleigh (4) derives the following relationship between the final collapse radius and the initial gas content, Q_o:

$$P_o \left[1 - \left(\frac{R_f}{R_m} \right)^3 \right] + Q_o \log_e \left(\frac{R_f}{R_m} \right)^3 = 0$$

$$\left(\frac{R_f}{R_m} \right)^3 << 1$$

$$\log_e \left(\frac{R_f}{R_m} \right)^3 = - \frac{P_o}{Q_o}$$

$$\left(\frac{R_m}{R_f} \right)^3 = e^{\frac{P_o}{Q_o}} \qquad [6]$$

Assuming adiabatic compression, Noltingk and Nepperas (9) derive the following relationship:

$$\left(\frac{R_m}{R_f}\right)^3 = \left[\frac{Q_o}{P_o}\left(\frac{k}{k-1}\right)\right]^{\frac{1}{(1-k)}} \qquad [7]$$

where k is the ratio of specific heats for the permanent gas inside the bubble. The value of k for air is 4/3. If the gas is air, then for adiabatic compression,

$$\left(\frac{R_m}{R_f}\right)^3 = \left(\frac{P_o}{4Q_o}\right)^3 . \qquad [7a]$$

Hence

$$p_c\Big|_{\text{isothermal}} = \frac{P_o}{6.35}\, e^{\frac{P_o}{Q_o}} ; \qquad [8]$$

$$p_c\Big|_{\text{adiabatic}} = \frac{P_o}{6.35}\left(\frac{P_o}{4Q_o}\right)^3 . \qquad [9]$$

Equations [8] and [9] are graphically shown in Figure 4. It is clear that the maximum collapse pressure and hence the intensity of collapse depends on whether the bubble collapse is isothermal or adiabatic. The Plesset-Hsieh criterion (5), (10) for the collapse of bubbles is as follows:

$$\text{Isothermal} \quad \text{if} \quad \frac{\rho_\ell S_\ell \Lambda_\ell}{\rho_g S_g R_m} \gg 1 \qquad [10]$$

$$\text{Adiabatic} \quad \text{if} \quad \frac{\rho_\ell S_\ell \Lambda_\ell}{\rho_g S_g R_m} \ll 1 \qquad [11]$$

where

ρ is the density,

S is the specific heat per unit mass , and

Λ is the thermal diffusion length .

and subscripts ℓ and g stand for liquid and gas respectively. Physically speaking, the above criteria give the relationship between the heat capacity of the gas inside the bubble and the heat that can be conducted away in the thermal diffusion layer of the liquid. If the latter is very large compared to the former, the temperature within the bubble remains constant. If it is very small then the temperature of the gas inside the bubble will rise. This criterion is shown in Figure 5 for various test liquids. The thermodynamic data were obtained from Reference 11 and the data for argon was obtained from Reference 12. At 20 kcs frequency, bubbles of maximum radii of a millimeter or less will be under isothermal compression while collapsing, for all the liquids shown in Figure 5. For larger bubble sizes, the collapse would become adiabatic. For this reason, the model-prototype correlation should take into account the Plesset-Hsieh criteria. However as seen in Figure 4, adiabatic collapse produces much less pressures and may not be important as far as cavitation damage is concerned.

Gas content of the bubble - The partial pressure of the gas inside the bubble at its maximum radius, Q_o (in Equations [8] and [9]) consist of three components:

1. The gas content at the beginning of the bubble growth, i.e., the gas inside the equilibrium nucleus of radius R_n.
2. The gas dissolved in the evaporated liquid during growth.
3. The gas that diffuses into the bubble from the surrounding liquid during growth.

Hence the partial pressure at the start of the collapse, Q_o, will be the sum total of the three components stated above.

$$Q_o = Q_1 + Q_2 + Q_3 \qquad [12]$$

1. Estimation of Q_1: The equation of static equilibrium for spherical bubbles is given by

$$P_o + \frac{2\gamma}{R_n} = p_v + p_g$$

where

P_o is the pressure in the surrounding liquid,

R_n is the equilibrium radius of the nucleus,

γ is the surface tension of the liquid,

p_v is the vapor pressure of the liquid, and

p_g is the partial pressure of the gas.

Hence

$$p_g = \left(P_o + \frac{2\gamma}{R_n} - p_v \right) .$$

Assuming the gas inside the nucleus to be a perfect gas,

$$p_g \frac{4}{3} \pi R_n^3 = N_1 \theta T_a$$

where

N_1 is the number of moles of the gas ,

θ is the perfect gas law constant , and

T_a is the absolute ambient temperature .

$$N_1 = \frac{p_g \frac{4}{3} \pi R_n^3}{\theta T_a}$$

$$= \frac{\left(P_o + \frac{2\gamma}{R_n} - p_v \right) \frac{4}{3} \pi R_n^3}{\theta T_a} .$$

The partial pressure, Q_1, exerted by these molecules when the nucleus grows to a maximum radius, R_m, is given by

$$Q_1 \frac{4}{3} \pi R_m^3 = N_1 \theta T_a$$

$$Q_1 = \left(P_o + \frac{2\gamma}{R_n} - p_v \right) \left(\frac{R_n}{R_m} \right)^3 . \qquad [13]$$

2. Estimation of Q_2 : The mass of liquid evaporated during growth, is equal to the mass of vapor in the bubble and is given by

$$m_\ell = \frac{4}{3} \pi R_m^3 \rho_v$$

where

m_ℓ is the mass of liquid evaporated

ρ_v is the density of vapor inside the bubble

The mass of gas which was originally dissolved in this mass of liquid before evaporation is

$$m_g = \alpha_g m_\ell = \frac{4}{3} \pi R_m^3 \rho_v \alpha_g$$

where α_g is the mass fraction of gas dissolved in the liquid. The number of moles of gas in this mass is given by

$$N_2 = \frac{m_g}{M_g} = \frac{4}{3} \pi R_m^3 \rho_v \frac{\alpha_g}{M_g}$$

where M_g is the molecular weight of gas. Similarly the number of moles of vapor N_v is given by

$$N_v = \frac{\frac{4}{3}\pi R_m^3 \rho_v}{M_v}$$

where M_v is the molecular weight of vapor.

$$\frac{N_a}{N_v} = \frac{\alpha_g M_v}{M_g}$$

Assuming the perfect gas law to be valid both for gas and vapor

$$Q_a \frac{4}{3} \pi R_m^3 = N_a \theta T_a$$

$$p_v \frac{4}{3} \pi R_m^3 = N_v \theta T_a$$

where

Q_a is the partial pressure of the gas exerted by N_a gas molecules

p_v is the vapor pressure inside the bubble

$$\frac{Q_a}{p_v} = \frac{N_a}{N_v} = \alpha_g \frac{M_v}{m_g}$$

$$Q_a = p_v \alpha_g \frac{M_v}{M_g} \qquad [14]$$

3. Estimation of Q_a: While the bubble grows from an equilibrium nucleus to a maximum radius R_m, the gas dissolved in the liquid with a partial pressure of P_o will diffuse into the bubble from a gas diffusion layer surrounding the bubble and is given by Bebchuck (13) as

$$Q_3 = \alpha_g P_o \frac{(D_g t)^{\frac{1}{2}}}{R_m} \qquad [15]$$

where

α_g is the concentration of the dissolved gas,

D_g is the diffusivity of the gas,

t is the diffusion time, and

$(D_g t)^{\frac{1}{2}}$ is the gas diffusion layer thickness.

Now the partial pressure of the gas inside the bubble at the beginning of collapse is given by Equation [12] which becomes

$$Q_o = Q_1 + Q_2 + Q_3$$

$$= \left(P_o + \frac{2\gamma}{R_n} - p_v\right)\left(\frac{R_n}{R_m}\right)^3 + p_v \alpha_g \frac{M_v}{M_g} + P_o \alpha_g \frac{(D_g t)^{\frac{1}{2}}}{R_m}$$

$$\frac{Q_o}{P_o} = \left[1 + \frac{2\gamma}{P_o R_n} - \frac{p_v}{P_o}\right]\left(\frac{R_n}{R_m}\right)^3 + \frac{p_v}{P_o}\alpha_g \frac{M_v}{M_g} + \alpha_g \frac{(D_g t)^{\frac{1}{2}}}{R_m}\Bigg] .$$

Since (R_n/R_m) is usually small compared to unity, the first term on the right hand side of the above equation is negligible compared to the other two terms. Then

$$\frac{Q_o}{P_o} \simeq \frac{p_v}{P_o}\,\alpha_g\,\frac{M_v}{M_g} + \alpha_g\,\frac{(D_g t)^{\frac{1}{2}}}{R_m} \qquad [16]$$

At temperatures much lower than the boiling point of the liquid, the vapor pressure is small. Hence

$$\frac{p_v}{P_o} << 1$$

$$\frac{M_v}{M_g} \quad \text{is of the order of 1}$$

If we assume that the gas diffusion layer, $(D_g t)^{\frac{1}{2}}$, is of the same order of magnitude as R_m, then the Equation [16] may be written as follows:

$$\frac{Q_o}{P_o} \cong \alpha_g\,\frac{(D_g t)^{\frac{1}{2}}}{R_m} \qquad [17]$$

However at temperatures close to the boiling point of the liquid, the vapor itself might act as a damper since the vapor may not fully condense during collapse. This effect will be discussed next.

C. Thermal Effects

The next important aspect that controls the collapse of vapor bubbles is the heat outflow during collapse. The heat of condensation is given in (5) as

$$H = \frac{4}{3}\pi R_m^3 \rho_v L$$

where

ρ_v is the density of vapor, and

L is the latent heat of vaporization.

This heat flows into the thermal diffusion layer of thickness $(Dt)^{\frac{1}{2}}$ where D is the thermal diffusivity and t is the time of collapse. The heat balance is given by

$$\frac{4}{3}\pi R_m^3 \rho_v L \cong 4\pi R_m^2 (Dt)^{\frac{1}{2}} \rho_\ell S_\ell \Delta T$$

$$\Delta T \cong \frac{R_m L \rho_v}{3(Dt)^{\frac{1}{2}} S_\ell \rho_\ell}$$

$$\frac{\Delta T}{T_B} = \frac{R_m L \rho_v}{3(Dt)^{\frac{1}{2}} S_\ell \rho_\ell T_B} \qquad [18]$$

where

ΔT is temperature difference between the liquid and the vapor,

T_B is the boiling point of the liquid at atmospheric pressure, and

S_ℓ is the specific heat of liquid per unit mass.

Assuming a millimeter for R_m and 20 μ seconds for growth or collapse time in various liquids tested Figure 6 shows that the

relative temperature difference increases sharply at temperatures closer to the boiling points of the liquids. Thermodynamic data are obtained from References 11 and 12.

Furthermore Plesset (5) has shown that

$$v = \dot{R}\left[1 - \frac{\rho_v}{\rho_\ell}\left(1 - \frac{v'}{\dot{R}}\right)\right]$$

where

$\dot{R} = \frac{dR}{dt}$ is the velocity of the bubble wall, i.e., the interface

v is the velocity of the liquid adjacent to the interface, and

v' is the velocity of the vapor adjacent to the interface.

Since ρ_v/ρ_ℓ is very small, it is evident that v is very nearly equal to $\dot{R}$ for most practical cases.

Relative importance of dissolved gas content and vapor pressure - From the above discussion, it is clear that when $\Delta T/T_B$ is small, the damping is entirely due to the dissolved gas content in the liquid. When $\Delta T/T_B$ is increasing with ambient temperature, the vapor itself may act as a damper. At these temperatures the vapor pressure of the liquids become important.

D. Compressibility Effects

According to the Rayleigh bubble collapse mechanism, the kinetic energy of bubble collapse is stored in the bulk compressibility of the liquid and transmitted back to the material in the

form of a short range shock. In order to investigate the compressibility effects, we need the Mach number of the bubble collapse. However, there are three sound speeds that are to be considered:

1. The sound speed in the liquid
2. The sound speed in the liquid-bubble mixture
3. The sound speed in the gas within the bubble

The Mach number M_w, may be defined as

$$M_w = \frac{\dot{R}}{C} \qquad [19]$$

where $\dot{R}$ is the bubble wall velocity and C is any of the sound speeds that is important. If we again consider the Rayleigh bubble collapse, then $\dot{R}$ is given by

$$\dot{R} = \sqrt{\frac{2}{3}\frac{P_o}{\rho}\left[\left(\frac{R_m}{R_f}\right)^3 - 1\right]}$$

Since $\left(\frac{R_m}{R_f}\right)^3 >> 1$

$$\dot{R} = \sqrt{\frac{2}{3}\frac{P_o}{\rho}\left(\frac{R_m}{R_f}\right)^3}$$

From Equations [6] and [7a]

$$\left.\begin{aligned} \dot{R} &= \sqrt{\frac{2}{3}\frac{P_o}{\rho}\, e^{\frac{P_o}{Q_o}}} && \text{For isothermal collapse} \\ \dot{R} &= \sqrt{\frac{2}{3}\frac{P_o}{\rho}\left(\frac{P_o}{4Q_o}\right)^3} && \text{For adiabatic collapse} \end{aligned}\right\} \quad [20]$$

During the analysis of experimental results, the effect of these physical parameters will have to be considered.

E. Surface Tension Effects

The surface tension effects may be scaled by the Weber number, W_w, for the motion of bubble wall given by

$$W_w = \frac{\rho_\ell (\dot{R})^2 R_m}{2\gamma} \quad [21]$$

F. Viscous Effects

Similarly if viscous effects were to become important in the bubble motions during growth and collapse, then the corresponding Reynolds number, R_w, for the bubble motion will be given by

$$R_w = \frac{\dot{R}\, R_m}{\nu} \quad [22]$$

where ν is the kinematic viscosity of the liquid.

EFFICIENCY OF CAVITATION DAMAGE

As pointed out in the introduction, the efficiency of cavitation damage will depend upon the various physical effects that control the maximum collapse pressure. The efficiency of cavitation damage may be defined as

$$\eta = \frac{I_d}{I_c} = \frac{\frac{i\,S_e}{t}}{\frac{p_c^2}{\rho_\ell C_\ell}}$$

From the previous discussion,

$$\frac{p_c}{p_o} = F_1\left(\Gamma_g,\ \frac{p_v}{p_o},\ \frac{(D_g t)^{\frac{1}{2}}}{R_m},\ \frac{\Delta T}{T_B},\ M_w,\ W_w,\ R_w,\ \text{Flow Parameters}\right)$$

Hence

$$\eta = \frac{\frac{i\,S_e}{t}}{\frac{P_o^2}{\rho_\ell C_\ell}} = F_2\left(\Gamma_g,\ \frac{p_v}{p_o},\ \frac{(D_g t)^{\frac{1}{2}}}{R_m},\ \frac{\Delta T}{T_B},\ M_w, W_w, R_w,\ \text{Flow Parameters}\right). \qquad [23]$$

It would be interesting to see which non-dimensional parameters in Equation [23] really influence the efficiency of cavitation damage for a typical experimental apparatus. One of the most widely used equipments for studies on cavitation damage is the magnetostriction vibratory apparatus. What follows is a discussion of the correlation of the experimental data obtained with this apparatus.

CORRELATION OF EXPERIMENTAL RESULTS OF VIBRATORY TESTS

The basic idea in these experiments is to vibrate a test specimen in a given liquid contained in a beaker at a given amplitude and frequency (see Figure 7). These vibrations are produced in most cases by the magnetostriction oscillators. Since 1935 several authors (e.g. References 14 through 19) have conducted these tests for investigating the phenomenon of cavitation damage. The basic parameters involved in these tests are the beaker dimensions, the specimen dimensions, amplitude and frequency of vibrations, the physical and chemical properties of the material and liquid used. The present analysis is confined to relatively non-corrosive liquids and metals. Only physical mechanisms are assumed to play any role.

When a cylindrical piston vibrates with its circular face inside the liquid as shown in Figure 7a the maximum pressure P_o is given (Reference 20) by

$$P_o = \rho_\ell C_\ell U_o \qquad [24]$$

where

$U_o = \omega_o \xi_o$,

$\xi = \xi_o \sin \omega_o t$,

ξ is the amplitude of vibration at any time t,

ξ_o is the maximum amplitude of vibration, and

ω_o is the angular frequency of vibration.

For a geometrically similar non-cavitating system, the maximum pressure depends upon the frequency parameter, μ, given by

$$\mu = \frac{2\pi a}{\lambda_\ell}$$

where a is the radius of the test specimen and λ_ℓ is the wave length of sound in the liquid. At this juncture, it is important to recognize the following fact pointed out by Phillips.* It is generally observed during experiments with the vibratory apparatus that there is a rim of area (at the periphery of the eroded surface) which does not get eroded at all in soft aluminum (see Figure 7b). The thickness of the rim is indeed of the order of one-half wave length as pointed out by Phillips if we use a value of about 100 fps for the sound speed at 14000 cps oscillations. This magnitude of sound speed is typical for air-water mixtures. Here again the importance of the compressibility of the two phase mixtures is evident. If this were to be true, then the measurement of rim thickness would give the magnitude of sound speeds in cavitation bubble mixtures. For this case Equation [23] may be written as

$$\eta = \frac{\frac{iS_e}{t}}{\rho_\ell C_\ell U_o^2}$$

$$= F\left[\Gamma_g,\ \frac{p_v}{P_o},\ \frac{(D_g t)^{\frac{1}{2}}}{R_m},\ \frac{\Delta T}{T_B},\ M_w,\ W_w,\ R_w,\ \mu\right] \qquad [25]$$

---

* O.M. Phillips, personal discussion with the author.

where

Γ_g	is the volume concentration of dissolved gas (damping due to gas content)
p_v/P_o	is the relative vapor pressure
$(D_g t)^{\frac{1}{2}}/R_m$	is the relative diffusion length
$\Delta T/T_B$	is the relative-bubble-wall-temperature-increase during collapse (thermal effects)
M_w	is the Mach number of the bubble wall motion (compressibility effects)
W_w	is the Weber number of the bubble wall motion (surface tension effects)
R_w	is the Reynolds number of the bubble wall motion (viscous effects)
and μ	is the frequency parameter.

The experimental results of several authors are shown in Figure 8 along with the range of variables involved in these tests. The rate of weight loss is plotted against temperature in the melting-boiling range for each liquid. All these experiments were conducted at atmospheric pressure except for one case in which Kerr and Leith (16) conducted experiments at 2.4 atmospheres absolute. The table attached to this figure gives all the available information on the liquid, material, amplitude, frequency and pressure used in these tests. These data provide substantial information to understand the relative importance of the various parameters contained in Equation [25]. The surface tensions of these liquids vary from 25 dynes/cm (for aniline) to 75 dynes/cm (for water), the viscosity from 0.3 centipoises to 10 centipoises,

the sound speed from 1320 meters/sec to 1650 meters/sec and the density from 0.8 gm/cm^3 to 1.0 gm/cm^3. These data were obtained from the International Critical Tables and from the Handbook of Physics and Chemistry.

The efficiency as given in Equation [25] was calculated from these data and plotted against the dissolved air content as shown in Figure 9. The rate of depth of erosion was obtained from rate of weight loss divided by the density of the material and the area of specimen. The rate of erosion is time dependent (1), (21), (22). Our experimental data were obtained in the steady state whereas all the other investigators did not separate the time effect. This is an obvious limitation. The erosion strength values for the metals have been obtained from previously published results. In some cases as indicated in Figure 9, an equivalent erosion strength has been used to take into account the time effect. For water the dissolved air content was measured with the Van Slyke apparatus. The dissolved air content decreases with testing time at a constant temperature in the vibratory tests as shown in Figure 10 and reaches a steady value. The steady value depends upon the test temperature as shown in Figure 11. In Figure 10, the published values of air content in water at various temperatures are also shown for comparison. The air content for aniline, toluene and benzene are given in International Critical Tables for room temperature. The air content was assumed to vary inversely as the temperature and was calculated for every other temperature as shown in Figure 11.

The rate of damage increases with temperature and then decreases with increasing temperature as shown in Figure 8. The peak damage occurs around 50 to 70 percent of the boiling point. As shown in Figure 6, in this temperature range the relative bubble wall temperature, $\Delta T/T_B$, seems to increase rapidly with the result that the vapor pressure also becomes important. All the data shown in Figure 9 are for the case when this effect is not important (i.e., when the ambient temperature is below the temperature that produces the peak damage). Above this temperature, the relative vapor pressure becomes the important correlating parameter as shown in Figure 12 in which the values of η/η_{peak} are plotted against p_v/P_o for water, benzene, toluene and aniline. Aniline seems to behave differently as compared to the other three liquids. One possible explanation is that the viscosity of aniline is one order of magnitude higher than that for the other three liquids. Viscous damping seems to be important at higher temperatures when vapor pressure plays a dominant role. However at lower temperatures the viscosity seems to be unimportant as shown by the correlation in Figure 9. This is further supported by the experiments with solutions of non-Newtonian additives shown in Figure 13. Vibratory cavitation damage tests were conducted in solutions of sodium carboxymethylcellulose. The concentrations of these additives were varied such that the viscosity of these solutions would vary tenfold. No noticeable change in rate of damage were observed at room temperature.

Considering the fact that the results presented in Figure 9 belong to a wide variety of data collected by different authors using different experimental conditions, the efficiency of damage seems to depend primarily on dissolved gas content of the liquid at temperatures well below the boiling point. Additional information presented in Figure 12 seems to indicate that the relative vapor pressure is also important at temperatures close to boiling point. The characteristic behavior of aniline indicates the importance of viscosity at higher temperatures. Additional questions as to whether the compressibility and surface tension effects are important or not remains to be verified by additional experiments since the range of values of surface tension and sound speeds in the present case considered are not wide enough. Furthermore, the gas content in the liquids must be actually measured while other properties are accurately controlled. Hence further investigations to refine these correlations and to check the significance of compressibility and surface tension effects are necessary.

However the correlations shown in Figures 9 and 12 already explain, a priori, a few of the significant experimental results that needed clarification.

1. For example, the variation of damage intensity with the square of the amplitude of motion ((21) and (23)) can be explained as follows. The intensity should be proportional to the square of the amplitude according to Equation [25] if all the terms on the right hand side of this equation remain constant and independent of the amplitude.

2. In hydrocarbon liquids such as benzene, toluene, aniline, etc., the intensity of damage is generally observed to be much lower as compared to water. This can be explained in terms of the higher solubility of air in hydrocarbon liquids.

3. Wilson and Graham (18) observed that the rate of damage strongly depended on the value of $\rho_\ell C_\ell$ (acoustic impedance of the liquid) and an explanation of this effect is obvious from the present analysis. The non-linearity in their correlation may be explained in terms of the variation in solubility of air in the various liquids they studied.

4. Another interesting observation by Wilson and Graham (18) is that the rate of damage did not vary with viscosity over a wide range in their experiments with water and glycerene mixtures at room temperature. This confirms our own experiments with non-Newtonian additives shown in Figure 13. These results verify that viscous effects are not important at lower temperatures.

5. The dependence of damage on temperature is generally explained (see for example (17) and (19)) as follows. At lower temperatures the damage increases with temperature because the solubility of air decreases with temperature. However at higher temperatures the vapor pressure becomes important in dampening the collapse of bubbles. These explanations are quantitatively demonstrated in Figures 9 and 12.

If we neglect the compressibility and surface tension effects, we may rewrite Equation [23] as

$$\eta = \frac{\frac{i\ S_e}{t}}{\frac{P_o^2}{\rho_\ell C_\ell}} = F\left(\Gamma_g\ ,\ \frac{p_v}{P_o}\ ,\ R_w\ ,\ \text{Flow Parameters}\right) \qquad [26]$$

When vapor pressure is not important

$$\eta = \frac{\frac{i\ S_e}{t}}{\frac{P_o^2}{\rho_\ell C_\ell}} = F\left(\Gamma_g,\ \text{Flow Parameters}\right) \qquad [27]$$

HYDRODYNAMIC CAVITATION DAMAGE

Now the question is how to make use of the correlations obtained for the vibratory tests to derive similar relationships governing the efficiency of cavitation damage in actual hydrodynamic flow systems. Equation [27] may be rewritten for this case as

$$\eta = \frac{\frac{i\ S_e}{t}}{\frac{P_o^2}{\rho_\ell C_\ell}} = F\left(\Gamma_g\ ,\ \sigma\ ,\ R_e\right) \qquad [28]$$

where

σ is the cavitation parameter and

R_e is the Reynolds number of the flow.

However the magnitude of the characteristic pressure field P_o that forces the bubble to collapse is not readily known. Let us consider a practical example shown in Figure 1 where cavitation damage is produced in the wake of a circular cylinder. The Reynolds number and cavitation parameter will be given by

$$R_e = \frac{V_\infty D}{\nu}$$

and

$$\sigma = \frac{p_\infty - p_v}{\frac{1}{2}\rho_\ell V_\infty^2} \quad .$$

The turbulent pressure field would be given by

$$P_{o\ \text{turbulent}} \sim \tfrac{1}{2}\rho_\ell \overline{u'^2} \propto \tfrac{1}{2}\rho_\ell V_\infty^2 \qquad [29]$$

Similarly the stagnation pressure also will be given by

$$P_{o\ \text{stagnation}} \sim \tfrac{1}{2}\rho V_\infty^2 \qquad [30]$$

where

V_∞ is the free stream velocity

p_∞ is the free stream pressure

$\overline{u'}$ is the mean turbulent velocity fluctuation, and

D is the diameter of the cylinder.

If either of the above two relationships were to be true, the intensity of damage should vary as the fourth power of the free stream velocity (see Figure 14). However, Knapp (24) found that the intensity of damage varied as the 6th power of the free stream velocity. The value of the exponent is known to vary from 5 to 7 according to Kerr and Rosenberg (25). Thiruvengadam (26) found that the exponent varied from 4.5 to 8.5 at a constant value of the cavitation parameter depending upon the cavitating body.

These considerations lead us to conclude that an entirely different approach may be needed to explain the high power dependency on velocity. Lighthill (27, 28) analyzed the mechanism of conversion of energy from kinetic energy of fluctuating shearing motions (Reynolds stresses) into the acoustic energy of fluctuating longitudinal motions and derived the following equation from dimensional analysis:

$$I_a \sim \rho_\ell C_\ell V_\infty^2 \left(\frac{V_\infty}{C_\ell} \right)^6 \qquad [31]$$

where I_a is the acoustic intensity radiated by the turbulent eddies acting as quadrupole sources. If we assume that the cavitation bubbles get entrained by these eddies, then the eddies would correspond to oscillators driving the bubbles to collapse (Figure 14). Then just as in vibratory tests the efficiency of damage may be written as

$$\eta = \frac{\frac{i\, S_e}{t}}{\rho_\ell C_\ell V_\infty^2 M^6} \qquad [32]$$

where M is the Mach number of the flow. There are no systematic experimental data available to check the validity of the above relationships.

Furthermore cavitation damage also depends strongly on the value of the cavitation parameter at a given velocity (29, 26). Intensity of damage is maximum for a specific σ value at any given velocity. These considerations indicate that two sets of curves are necessary in order to predict a model prototype relationship as shown in Figure 15. The proposed method of model testing needs verification.

CONCLUSIONS

The following conclusions may be drawn from the previous analyses:

1. The intensity of bubble collapse is defined as the power radiated per unit surface area of the bubble. It is given by the square of the collapse pressure divided by the acoustic impedance of the liquid.

2. The efficiency of damage is defined as the ratio of the intensity of cavitation damage to the intensity of bubble collapse.

3. In the vibratory tests, the efficiency of damage is primarily controlled by the isothermal damping of the dissolved non-condensible gases at lower ambient temperature of the liquid. At higher temperatures closer to the boiling point, the vapor of the liquid itself plays an important role. This is because the relative bubble wall temperatures increase rapidly at these temperatures.

4. When the vapor pressure is important, the viscosity of the fluid also seems to be important as shown by the behavior of aniline.

5. Within the range of tests, the efficiency of damage seems to be independent of the surface tension of the liquid.

6. The above results of the vibratory tests have been extrapolated to propose a modeling technique to predict the intensity of cavitation damage in actual hydrodynamic systems. The proposed modeling technique needs experimental verification.

REFERENCES

1. Thiruvengadam, A., "A Comparative Evaluation of Cavitation Damage Test Devices," HYDRONAUTICS, Incorporated Technical Report 233-2, November 1963. (See also Symp. Cavitation Research Facilities and Techniques, ASME Publication, New York, pages 157-164, May 1964).

2. Thiruvengadam, A., "Intensity of Cavitation Damage Encountered in Field Installations," HYDRONAUTICS, Incorporated Technical Report 233-7, February 1965. (See also Symp. Cavitation in Fluid Machinery, ASME Winter Annual Meeting, November 1965. Available at ASME Headquarters, New York).

3. Thiruvengadam, A., "The Concept of Erosion Strength," HYDRONAUTICS, Incorporated Technical Report 233-9, December 1965 (See also Symp. Erosion by Cavitation or Impingement, ASTM Annual Meeting, Atlantic City, New Jersey, June 1966. Available at ASTM Headquarters, Philadelphia, Penn.)

4. Reyleigh, Lord, "On the Pressure Developed in a Liquid During the Collapse of a Spherical Cavity," Phil. Mag. (6) 34, pp. 94-98, 1917.

5. Plesset, M. S., "Bubble Dynamics," Proc. Symp.'Cavitation in Real Liquids', General Motors Research Laboratories, Warren, Michigan, 1962, Ed. R. Davies, ElServier Publishing Company, 1964.

6. Hsieh, D-Y, "Some Analytical Aspects of Bubble Dynamics," Trans. ASME, Jour. Basic Engr., Vol. 87, D, No. 4, pp. 991-1005, 1965.

7. Eisenberg, P., "On the Mechanism and Prevention of Cavitation," David Taylor Model Basin Report 712, July 1950.

8. Naude', C F., and Ellis, A. T., "On the Mechanism of Cavitation Damage by Nonhemispherical Cavities Collapsing in Contact with a Solid Boundary," Trans. ASME, Jour. Basic Engr., D 83, 648, 1961.

9. Noltingk, B. E., and Neppiras, E. A., "Cavitation Produced by Ultrasonics," Proc. Phys. Soc. (Lond), B. 63, p. 683, 1950.

10. Plesset, M. S., and Hsieh, D-Y, "Theory of Gas Bubble Dynamics in Oscillating Pressure Fields," The Physics of Fluids, Vol. 3, No. 6, p. 882, 1960.

11. Kreith, F., "Principles of Heat Transfer," International Textbook Company, Scranton, Penn., 1962, pp. 535-539.

12. Jackson, C. C., Ed-in-Chief, Liquid Metals Handbook, 3rd Edition, Published by AEC and BuShips, U.S.A., 1955.

13. Bebchuck, A. S., "On the Problem of the Mechanism of Cavitation Damage to Solid Bodies," Jour. Acoustics, Vol. 3, p. 369(1957), Soviet Physics-Acoustics Vol. 3, p. 395, 1958.

14. Schumb, Walter C., Peters, H., and Milligan, Lowell H., "Cavitation Erosion of Metals," Metals and Alloys, pp. 126-131, May 1937.

15. Nowotny, Hans, "Destruction of Material Through Cavitation-Investigation with an Oscillator," 1942 (In German).

16. Kerr, S. Logan, and Leith, W. C., "A Review of Cavitation Damage by the Vibratory Method," Dominion Engineering Works, Ltd., 1955.

17. Bebchuck, A. S., "On the Problem of Cavitation Damage to Solid Bodies," Jour. Acoustics, 3, 1, 90-91, 1957, (Soviet Physics-Acoustics, p. 95).

18. Wilson, R. W., and Graham, R., "Cavitation of Metal Surfaces in Contact with Lubricants," Conference on Lubrication and Wear, The Institution of Mechanical Engineers, Paper 83, 1st-3rd October 1957.

19. Plesset, Milton S., and Devine, Robert E., "Temperature Effects in Cavitation Damage," Report No. 85-27, Division of Engr. and Appl. Sci., California. Inst. of Tech., April 1964.

20. Morse, P. M., Vibration and Sound, 2nd Edition, McGraw Hill Book Company, New York, 1948, p. 334.

21. Thiruvengadam, A., and Preiser, H. S., "On Testing Materials for Their Cavitation Damage Resistance," HYDRONAUTICS, Incorporated Technical Report 233-3, December 1963. (See also Jour. of Ship Research, Vol. 8, No. 3, December 1964).

22. Eisenberg, P., Preiser, H. S., and Thiruvengadam, A., "On the Mechanism of Cavitation Damage and Methods of Protection," Paper No. 6, Winter Annual Meeting, The Society of Naval Architects and Marine Engineers, November 1965.

23. Bebchuck, A. S., Borisov, J. I., and Rozenburg, L. D., "On the Problem of Cavitation Erosion," Acoustics Jour. 1958, pp. 372-373.

24. Knapp, R. T., "Recent Investigations of the Mechanics of Cavitation and Cavitation Damage," Trans. ASME, Vol. 77, pp. 1045-1054, 1955. (See also R. T. Knapp "Accelerated Field Tests of Cavitation Intensity," Trans. ASME, Vol. 80, pp. 91-102, 1958).

25. Kerr, S. L., and Rosenberg, K., "An Index to Cavitation Erosion by Means of Radio-Isotopes," Trans. ASME, Vol. 80, pp. 1308-1314, 1958.

26. Thiruvengadam, A., "Cavitation and Cavitation Damage," M. Sc. Thesis, Indian Institute of Science, Bangalore, 12, 1959.

27. Lighthill, M. J., "On Sound Generated Aerodynamically," Part I. General Theory, Proc. Roy. Soc. A. 211, 564, 1952.

28. Lighthill, M. J., "On Sound Generated Aerodynamically," Part II, Turbulence as a Source of Sound, Proc. Roy. Soc. A. 222, February 1954.

29. Shalnev, K. K., "Experimental Study of the Intensity of Erosion Due to Cavitation," Proc. Symp. on Cavitation in Hydrodynamics, N.P.L., (Teddington) H.M.S.O. Publication, p. 22-p.1, 1955.

KNOWN SCALING PARAMETERS

1. CAVITATION PARAMETER,

$$\sigma = \frac{P - P_v}{\frac{1}{2}\rho V^2}$$

2. REYNOLDS NUMBER $= \frac{VD}{\nu}$

UNKNOWN SCALING PARAMETERS

THEY SHOULD CONSIST OF:

MATERIAL PARAMETERS
LIQUID PARAMETERS
BUBBLE PARAMETERS

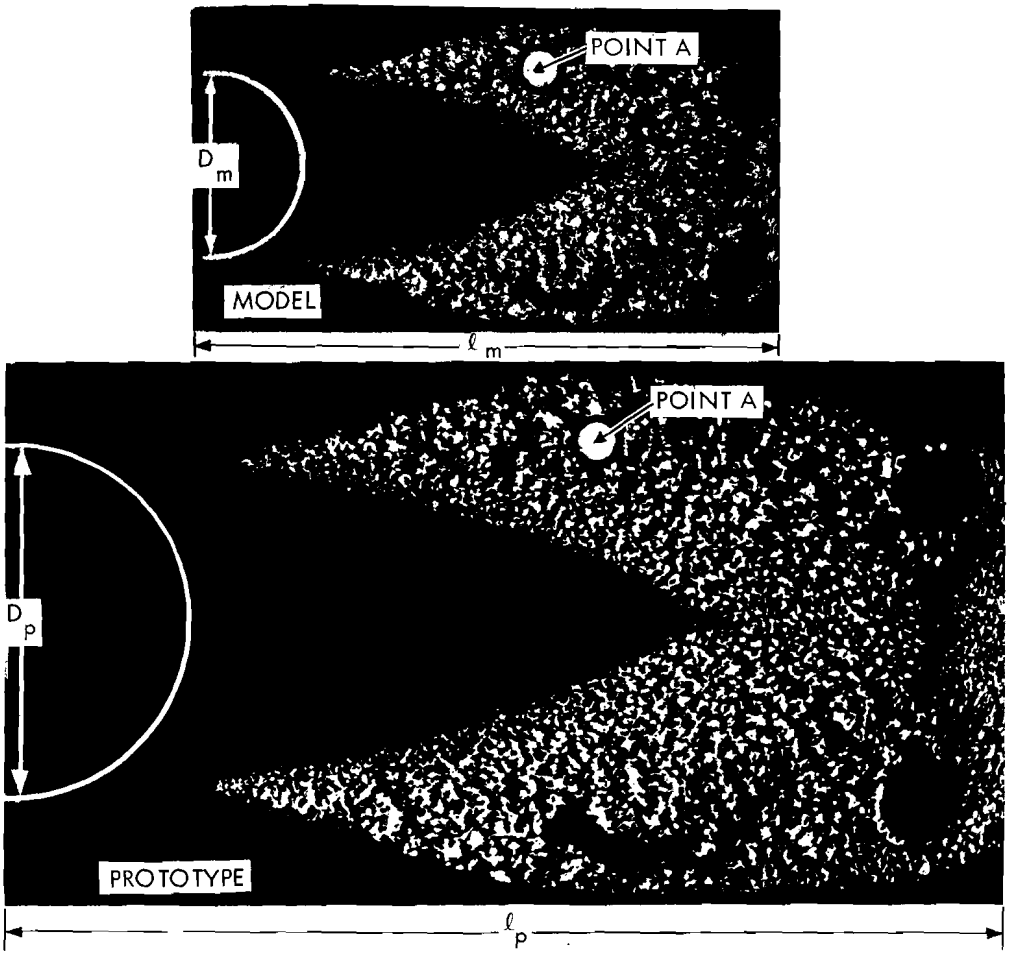

FIGURE 1 - PARAMETERS INVOLVED IN MODELING CAVITATION DAMAGE

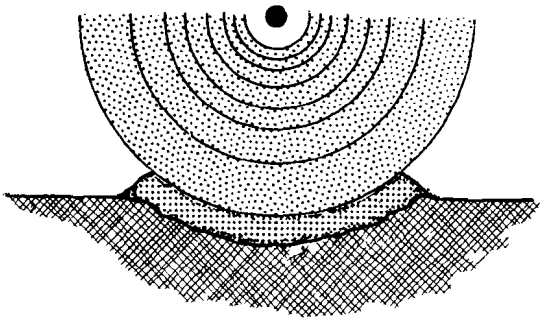

INTENSITY OF BUBBLE COLLAPSE $I_c = ?$

INTENSITY OF MATERIAL EROSION $I_d = \frac{iS_e}{t}$

EFFICIENCY $\eta = \frac{I_d}{I_c}$; WHAT ARE THE PARAMETERS THAT CONTROL THIS EFFICIENCY?

FIGURE 2 - PHASES OF ENERGY TRANSMISSION

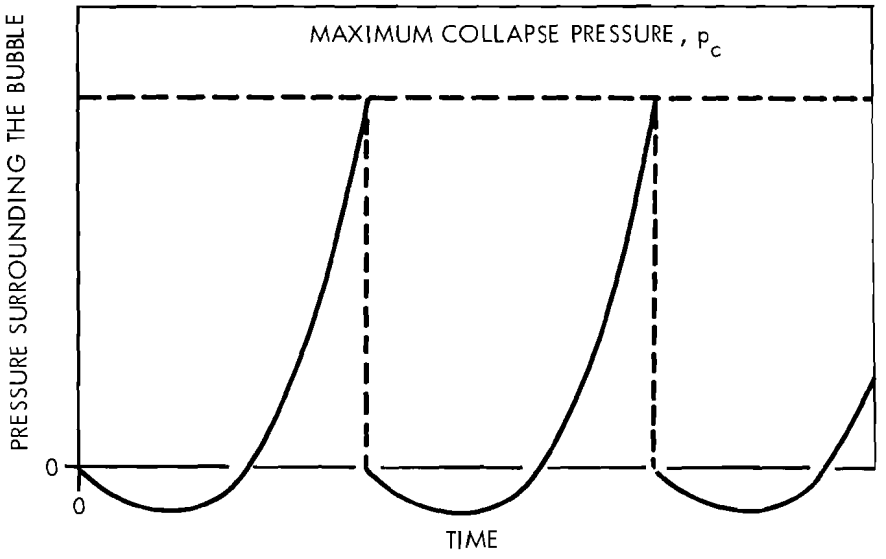

INTENSITY OF COLLAPSE $I_c = \frac{p_c^2}{\rho_\ell C_\ell}$

ρ_ℓ - LIQUID DENSITY

C_ℓ - SOUND SPEED IN LIQUID

FIGURE 3 - DEFINITION OF INTENSITY OF BUBBLE COLLAPSE

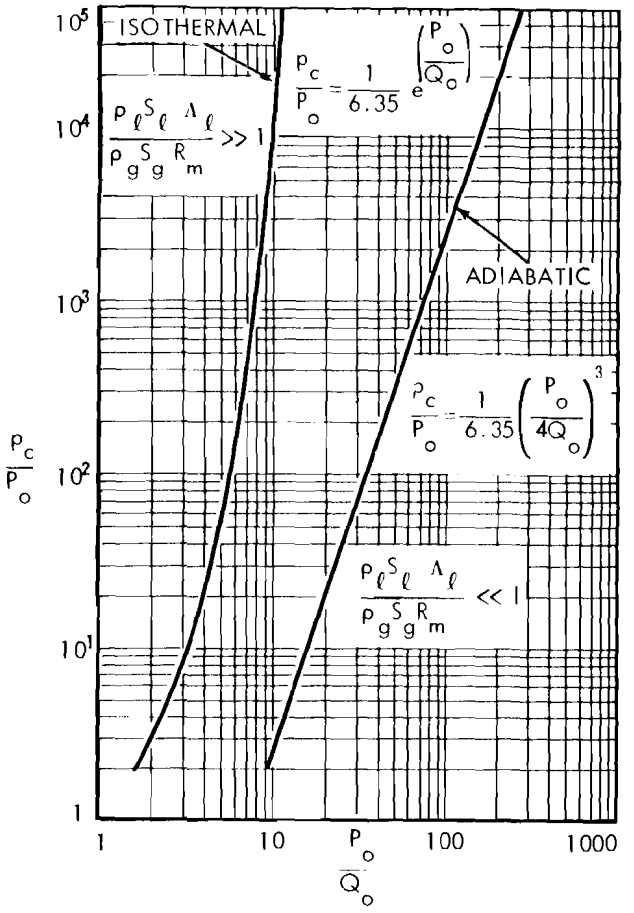

FIGURE 4 - BUBBLE COLLAPSE PRESSURES AS A FUNCTION OF GAS CONTENT BOTH FOR ISOTHERMAL AND FOR ADIABATIC DAMPING

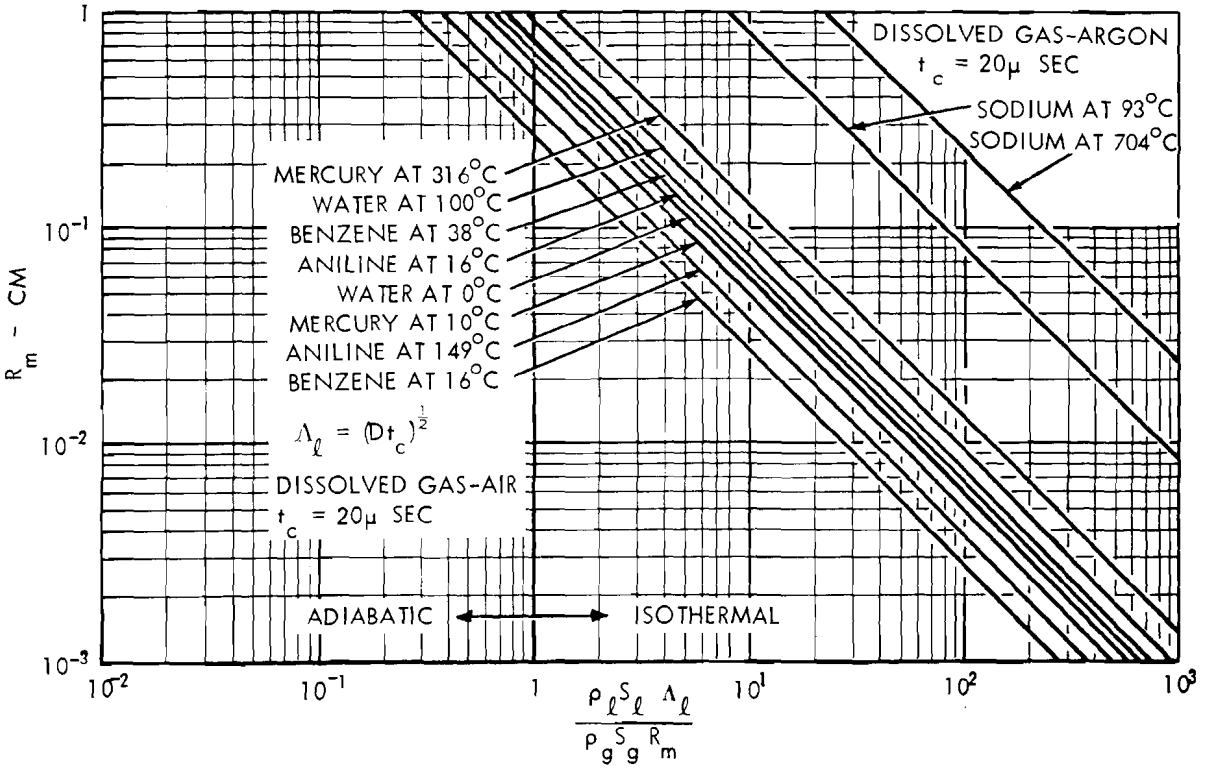

FIGURE 5 - PLESSET-HSIEH CRITERION FOR VARIOUS LIQUIDS TESTED

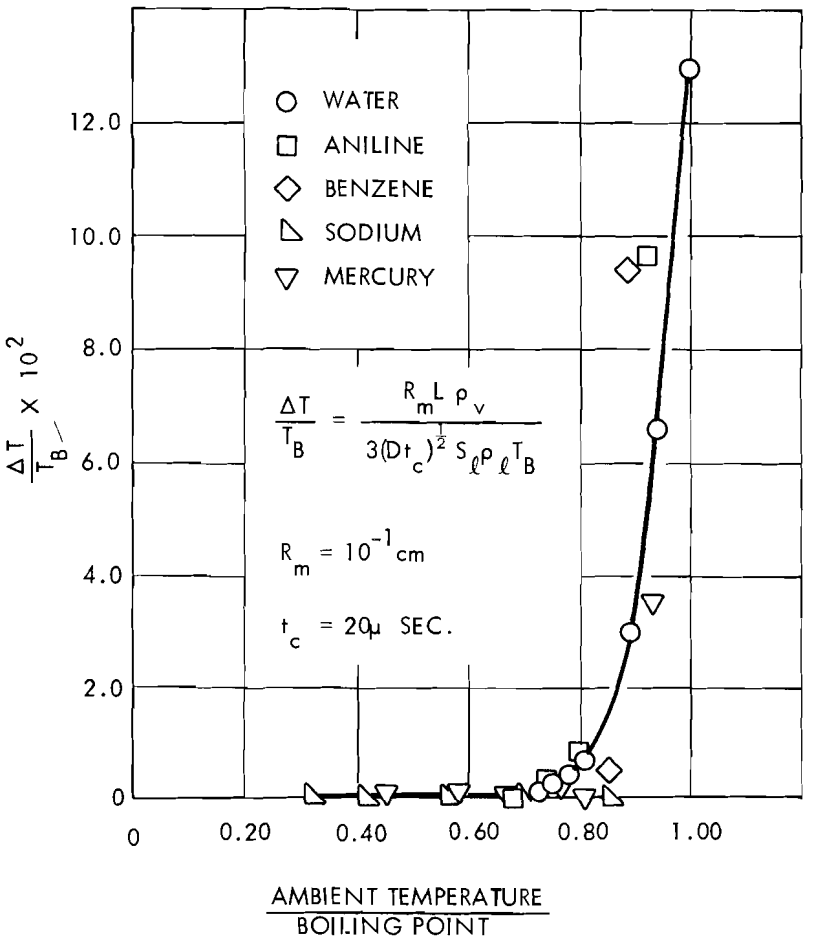

FIGURE 6 - THERMAL EFFECTS ON VAPOR BUBBLE GROWTH AND COLLAPSE

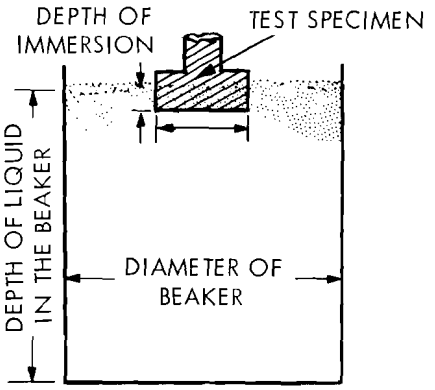

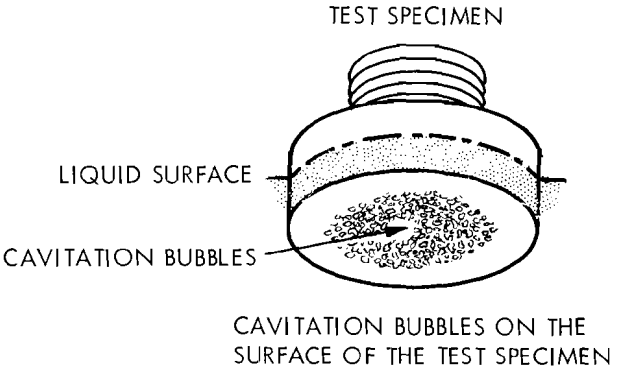

CAVITATION BUBBLES ON THE SURFACE OF THE TEST SPECIMEN

$$p_c = p_o F_1 (\Gamma_g)$$

$$I_c = \rho_\ell C_\ell U_o^2 F_2 (\Gamma_g)$$

$$I_d = \frac{iS_e}{t}$$

$$\eta = \frac{I_d}{I_c} = \frac{\frac{iS_e}{t}}{\rho_\ell C_\ell U_o^2}$$

$$\eta = F \left[\Gamma_g, \frac{\Delta T}{T_B}, M_W, W_W, R_W, \mu \right]$$

$\xi = \xi_o \sin \omega_o t$

$2\xi_o$ AMPLITUDE OF VIBRATION

ω_o ANGULAR FREQUENCY

$U_o = \omega_o \xi_o$

$P_o = \rho_\ell C_\ell U_o$

$I_a = \rho_\ell C_\ell U_o^2$

$\mu = \frac{2\pi a}{\lambda_\ell}$

(a)

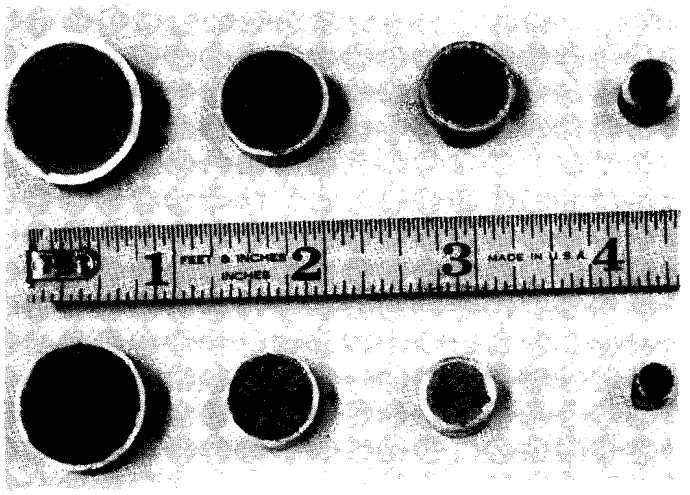

(b)

FIGURE 7 - PARAMETERS INVOLVED IN MODELLING VIBRATORY CAVITATION DAMAGE EXPERIMENTS

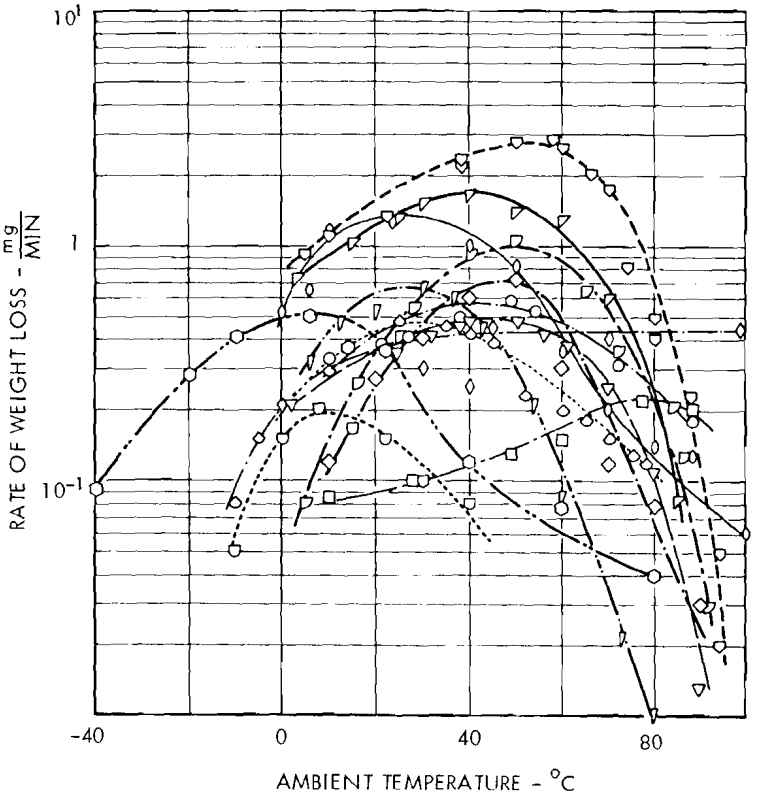

INVESTIGATOR	TEST MATERIAL	TEST LIQUID	FREQUENCY (kcs)	AMPLITUDE (mils)	PRESSURE ATMOS-PHERES	DATA SYMBOL	REF.
SCHUMB, PETERS AND MILLIGAM	ALUMINUM 51 - ST	WATER	8.7	1.97	1.0	▽	12
NOWOTNY	MAGNESIUM	WATER	9.0	1.18	1.0	◇	13
KERR AND LEITH	CAST IRON	WATER	6.5	1.71	1.0	○	14
	CAST IRON	WATER	6.5	1.71	2.4	□	14
BEBCHUCK	ALUMINUM	WATER	8.0	—	1.0	▽	15
	ALUMINUM	BENZENE	8.0	—	1.0	▽	15
	ALUMINUM	KEROSENE	8.0	—	1.0	◇	15
WILSON AND GRAHAM	WROUGHT ALUMINUM	ANILINE	12.0	—	1.0	◇	16
DEVINE AND PLESSET	ALUMINUM 2 /H 129	WATER	15.0	1.00	1.0	▽	17
WHITE	ALUMINUM	WATER	14.0	0.69	1.0	▽	*
	ALUMINUM	BENZENE	14.0	0.69	1.0	▽	*
	ALUMINUM	TOLUENE	14.0	0.69	1.0	⬡	*
	ALUMINUM	ANILINE	14.0	0.69	1.0	○	*

* DATA OBTAINED BY MRS. S. W. WHITE WITH THE HYDRONAUTICS' MAGNETOSTRICTION APPARATUS

LIQUID PROPERTY RANGE COVERED BY CAVITATION DAMAGE					
LIQUID	VAPOR PRESSURE dynes/cm^2	VISCOSITY Centipoises	SURFACE TENSION dynes/cm	DENSITY g/cm^3	VELOCITY OF SOUND m/sec
WATER	8.13×10^3 - 8.14×10^5	1.79 - 0.284	75.6 - 59.8	0.9998 - 0.9584	1431 - 1552
ANILINE	1.46×10^3 - 6.09×10^4	10.2 - 1.27	44.1 - 39.4	1.03893 - 0.97787	1643
BENZENE	6.06×10^4 - 7.27×10^5	0.758 - 0.329	30.2 - 25.0	0.88936 - 0.82466	1317
TOLUENE	1.37×10^4 - 3.86×10^5	0.772 - 0.354	27.7 - 25.0	0.92393 - 0.80913	1318

FIGURE 8 - SUMMARY OF RESULTS OF VIBRATORY TESTS

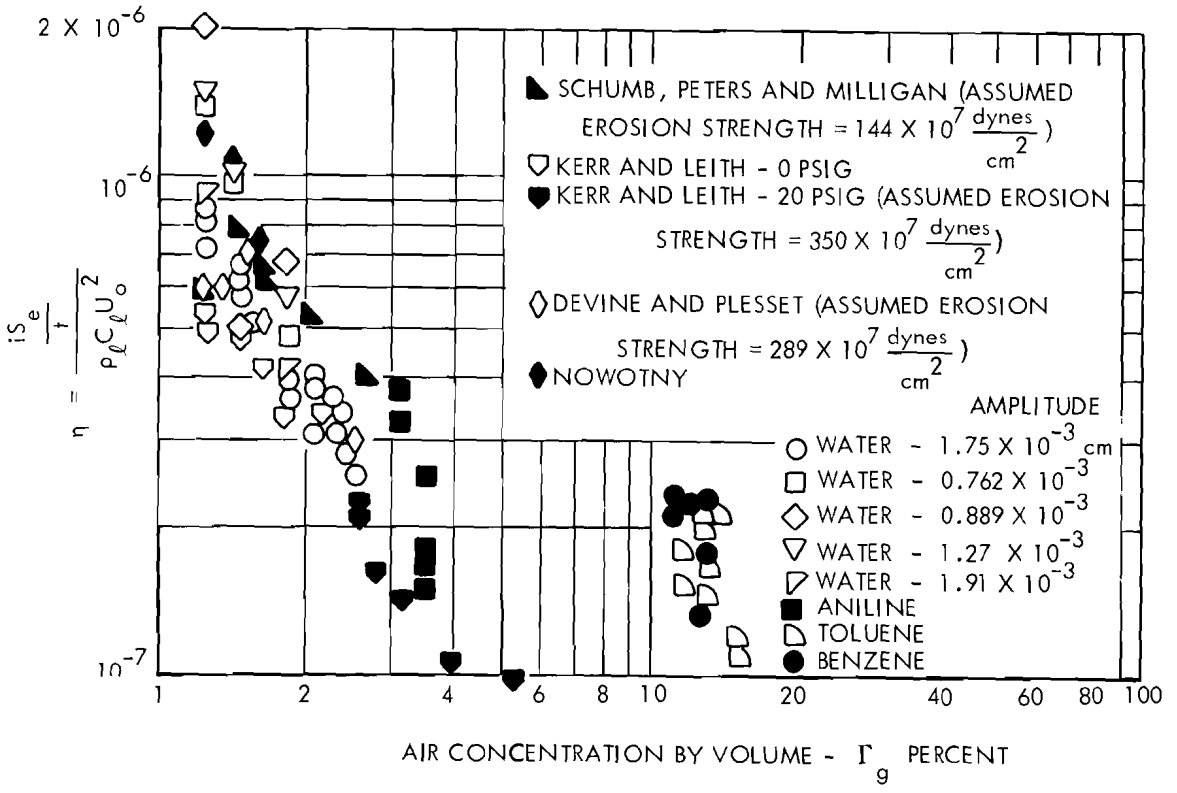

FIGURE 9 - CORRELATION OF EFFICIENCY OF DAMAGE WITH AIR CONCENTRATION IN VARIOUS LIQUIDS

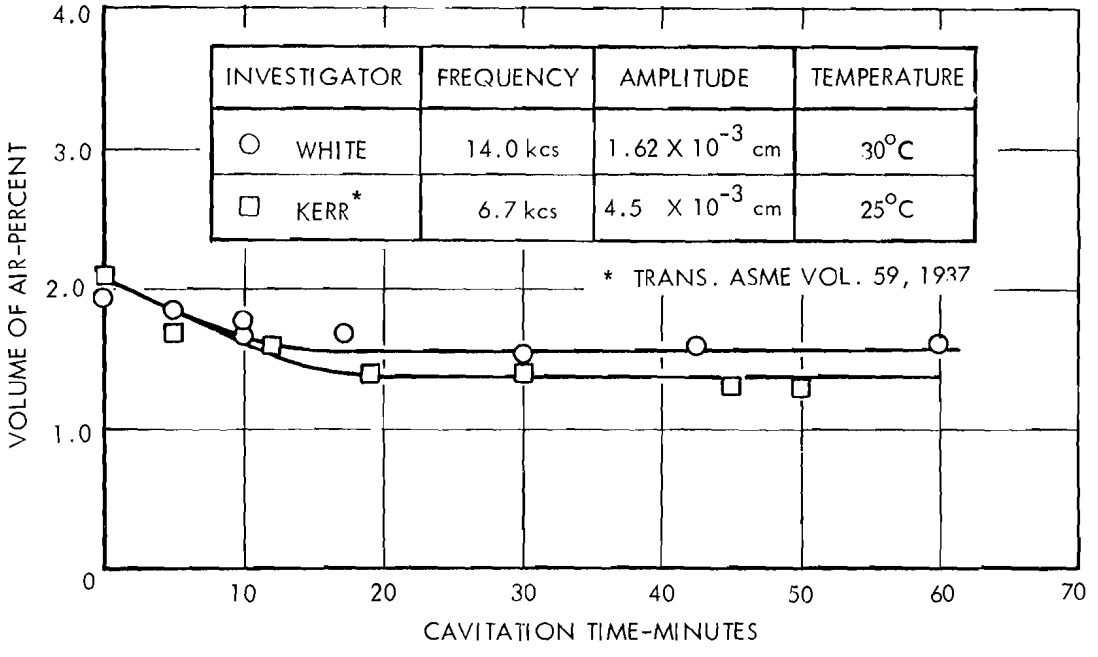

FIGURE 10 - VARIATION OF DISSOLVED AIR CONTENT WITH TEST DURATION IN VIBRATORY TEST

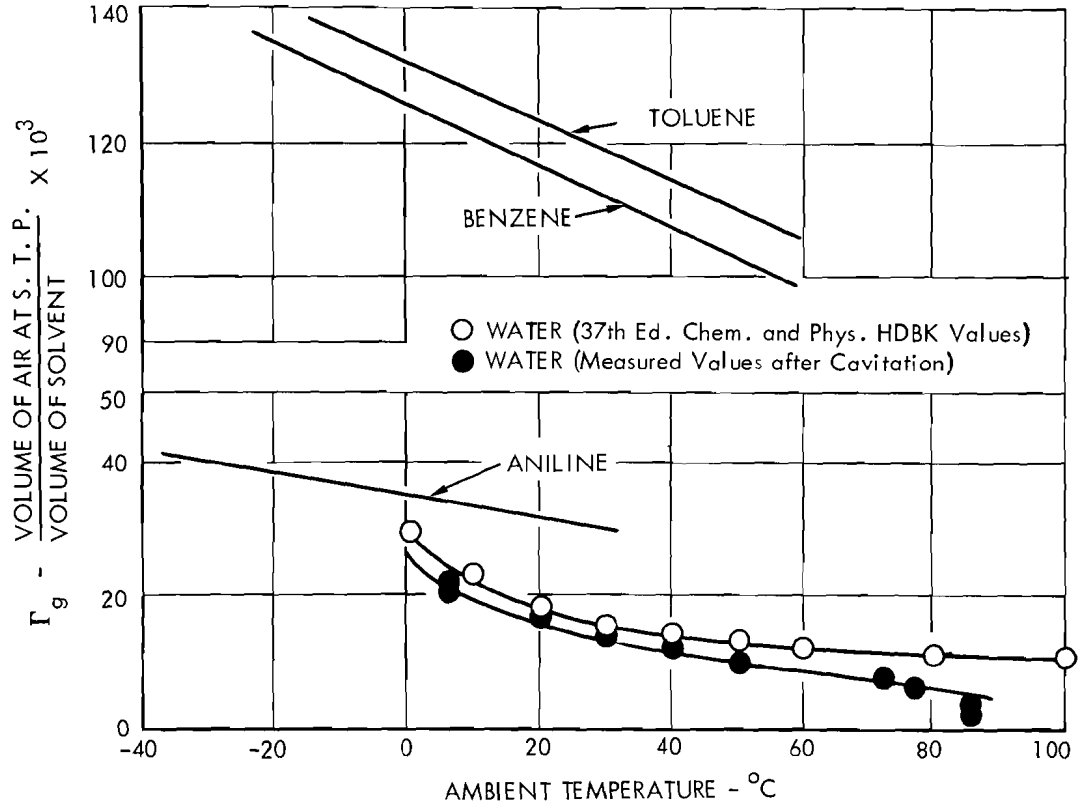

FIGURE 11 - DISSOLVED AIR CONTENT IN LIQUIDS

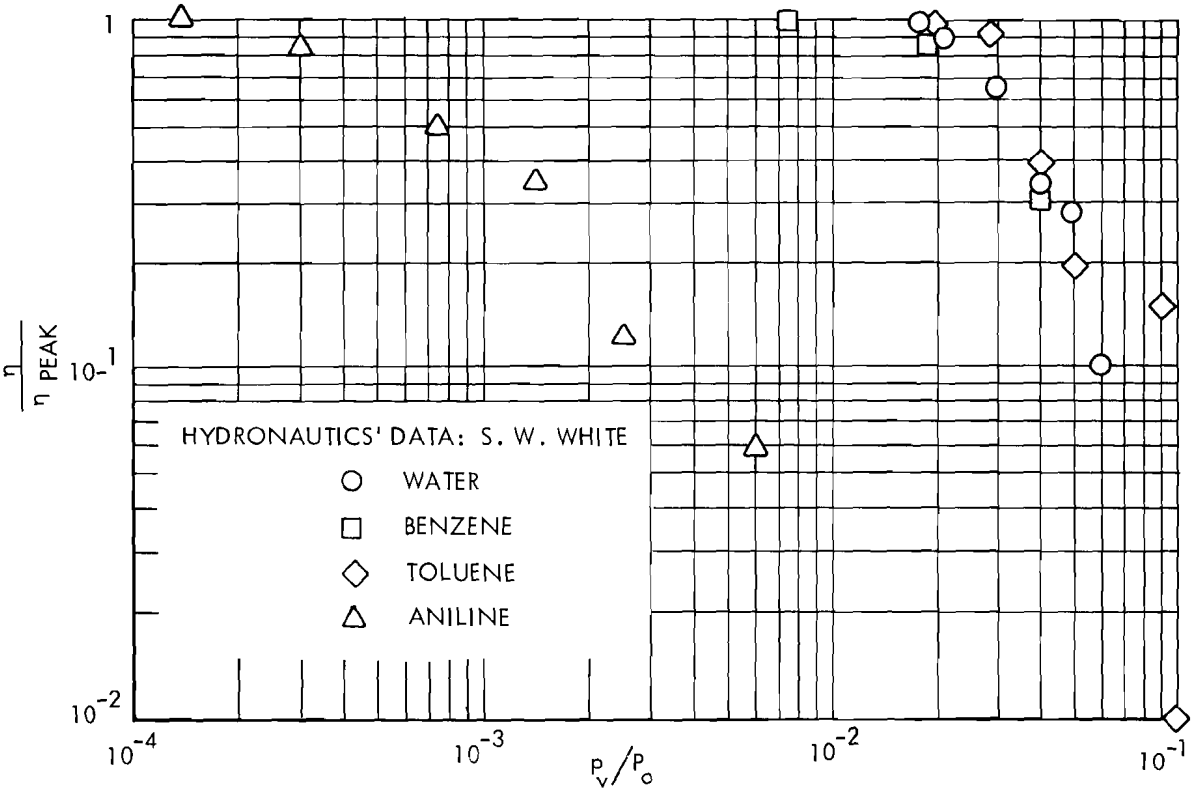

FIGURE 12 - CORRELATION OF EFFICIENCY WITH VAPOR PRESSURE AT TEMPERATURES CLOSE TO BOILING POINT

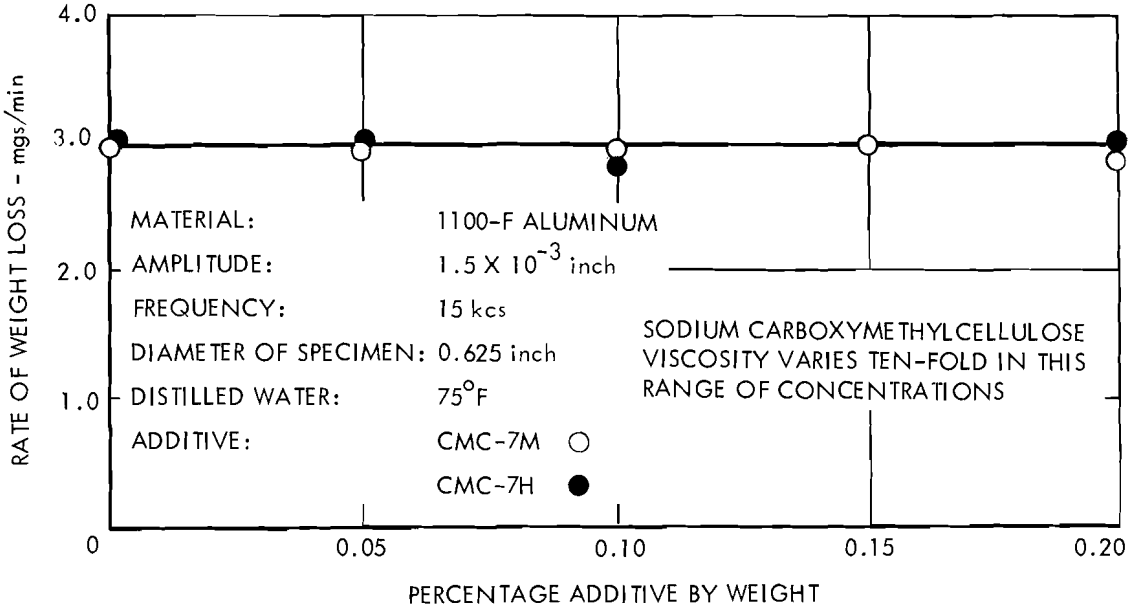

FIGURE 13 - EFFECT OF NON-NEWTONIAN ADDITIVE ON CAVITATION DAMAGE RATE

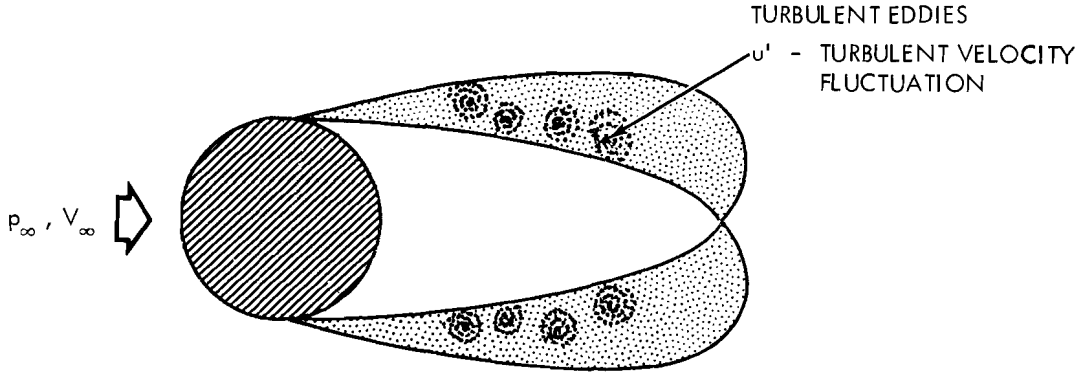

$$\eta = \frac{\frac{iS_e}{t}}{\frac{P_o^2}{\rho_\ell C_\ell}}$$

WHAT IS P_o?

A (a) TURBULENT PRESSURE FLUCTUATIONS

$$P_o \sim \tfrac{1}{2}\rho \bar{u}'^2 \quad \propto \tfrac{1}{2}\rho V_\infty^2$$

(b) TOTAL HEAD

$$P_o \sim p_\infty + \tfrac{1}{2}\rho V_\infty^2$$

THEN

$$I_c \sim \rho_\ell C_\ell V_\infty^2 \left(\frac{V_\infty}{C_\ell}\right)^2 \rightarrow V_\infty^4$$

B. LIGHTHILL'S QUADRUPOLE SOURCE MODEL

$$I_c \sim \rho_\ell C_\ell V_\infty^2 \left(\frac{V_\infty}{C_\ell}\right)^6 \rightarrow V_\infty^8$$

FIGURE 14 - HYDRODYNAMIC CAVITATION DAMAGE

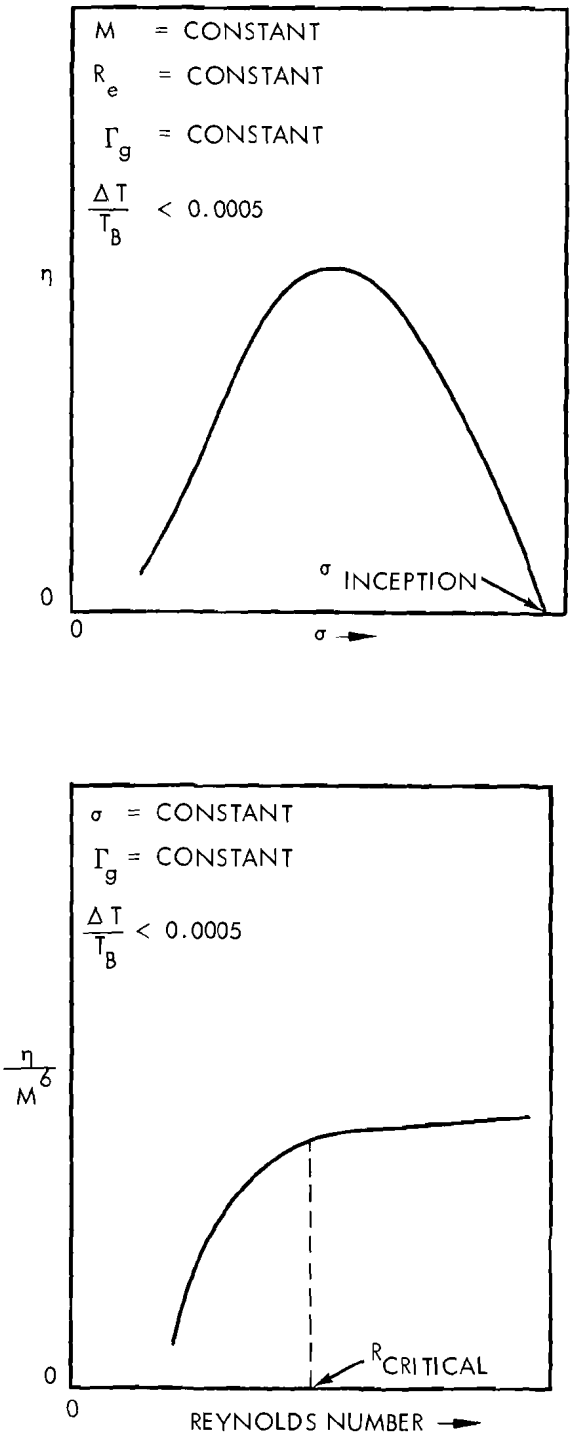

FIGURE 15 - PROPOSED METHOD OF MODELING CAVITATION DAMAGE

HYDRONAUTICS, Incorporated

DISTRIBUTION LIST
(Contract Nonr 3755(00))

Chief of Naval Research
Department of the Navy
Washington 25, D. C. 20360
Attn: Codes 438 — 3
461 — 1
463 — 1
429 — 1

Commanding Officer
Office of Naval Research
Branch Office
495 Summer Street
Boston 10, Massachusetts — 1

Commanding Officer
Office of Naval Research
Branch Office
219 S. Dearborn Street
Chicago, Illinois 60604 — 1

Commanding Officer
Office of Naval Research
Branch Office
207 West 24th Street
New York 11, New York 10011 — 1

Commanding Officer
Office of Naval Research
Branch Office, Box 39
Fleet Post Office
New York, 09510 — 25

Commanding Officer
Office of Naval Research
Branch Office
1030 East Green Street
Pasadena 1, California — 1

Director
U. S. Naval Research Lab.
Washington 25, D. C.
Attn: Codes 2000 — 1
2020 — 1
2027 — 6

Chief, Bureau of Ships
Department of the Navy
Washington 25, D. C.
Attn: Codes 300 — 1
305 — 1
335 — 1
341 — 1
342A — 1
345 — 1
421 — 1
440 — 1
442 — 1
634A — 1
634(B.Taylor) — 1
634(L.Birnbaum) — 1
430(L.Wechsler) — 1

Chief, Bureau of Naval Weapons
Department of the Navy
Washington 25, D. C.
Attn: Codes R — 1
R-12 — 1
RR — 1
RRRE — 1
RU — 1
RUTO — 1

Chief, Bureau of Yards and Docks
Department of the Navy
Washington 25, D. C.
Attn: Codes D-202 — 1
D-400 — 1
D-500 — 1

Commanding Officer and Director
David Taylor Model Basin
Washington 7, D. C.
Attn: Codes 142 1
500 1
513 1
521 1
526 1
550 1
563 1
589 1
Dr. M. Strasberg (901) 1

Commander
U. S. Naval Ordnance Laboratory
Silver Spring, Maryland
Attn: Dr. A. May 1
Desk DA 1
Desk HL 1
Desk DR 1

Commander
U. S. Naval Ordnance Test Station
China Lake, California
Attn: Codes 5014 1
4032 1
753 1

Hydrographer
U. S. Navy Hydrographic Office
Washington 25, D. C. 1

Commander
U. S. Naval Ordnance Test Station
Pasadena Annex
3202 E. Foothill Boulevard
Pasadena 8, California
Attn: Mr. J.W. Hoyt 1
Research Division 1
P508 1
P804 1
P807 1
P80962 (Library) 1
Mr. J.W. Hicks 1

Superintendent
U. S. Naval Academy
Annapolis, Maryland
Attn: Library 1

Commanding Officer and Director
U. S. Navy Marine Engr. Lab.
Annapolis, Maryland 21402
Attn: Code 750 1

Commander
U. S. Naval Weapons Laboratory
Dahlgren, Virginia
Attn: Tech. Library Div. 1
Computation and Exterior
Ballistics Laboratory
(Dr. Hershey) 1

Commanding Officer
NROTC and Naval Administrative
Unit, M.I.T.
Cambridge 39, Mass. 1

Commanding Officer and Director
U S. Underwater Sound Lab.
Fort Trumbull
New London, Connecticut
Attn: Technical Library 1

Commanding Officer and Director
U. S. Navy Mine Defense Lab.
Panama City, Florida 1

Superintendent
U. S. Naval Postgraduate School
Monterey, California
Attn: Library 1

Commanding Officer and Director
U. S. Naval Electronic Lab.
San Diego 52, California
Attn: Library 1

Commanding Officer and Director
U. S. Naval Civil Engr. Lab.
Port Hueneme, California 1

Commanding Officer and Director
U. S. Naval Applied Science Lab.
Brooklyn, New York 11251
Attn: Code 9370 1

Commander
Norfolk Naval Shipyard
Portsmouth, Virginia 1

Commander
New York Naval Shipyard
U. S. Naval Base
Brooklyn, New York 1

Commander
Boston Naval Shipyard
Boston 29, Massachusetts 1

Commander
Philadelphia Naval Shipyard
U. S. Naval Base
Philadelphia 12, Penn. 1

Commander
Portsmouth Naval Shipyard
Portsmouth, New Hampshire
Attn: Design Division 1

Commander
Charleston Naval Shipyard
U. S. Naval Base
Charleston, South Carolina 1

Commanding Officer
U. S. Naval Underwater Ordnance Station
Newport, Rhode Island
Attn: Research Division 1

Commander
Long Beach Naval Shipyard
Long Beach 2, California 1

Commander
Pearl Harbor Naval Shipyard
Navy No. 128 FPO
San Francisco, California 1

Commander
San Francisco Naval Shipyard
San Francisco 24, California 1

Shipyard Technical Library
Code 130L7, Bldg. 746
San Francisco Bay Naval Shipyard
Vallejo, California 94592 1

Superintendent
U. S. Merchant Marine Academy
Kings Point, L.I., New York
Attn: Dept. of Engr. 1

Commandant, U. S. Coast Guard
1300 E. Street, N. W.
Washington, D. C. 1

Beach Erosion Board
U. S. Army Corps of Engineers
Washington 25, D. C. 1

Commanding Officer
U. S. Army Research Office
Box CM, Duke Station
Durham, North Carolina 1

Commander
Hdqs. U. S. Army Transportation
Research and Development Command
Transportation Corps
Fort Eustis, Virginia 1

Director
U. S. Army Engineering Research
and Development Laboratories
Fort Belvoir, Virginia
Attn: Tech. Documents Center 1

Defense Documentation Center
Cameron Station
Alexandria, Virginia 20

Maritime Administration
441 G. Street, N. W.
Washington 25, D. C.
Attn: Coordinator of Research 1
Div. of Ship Design 1

Fluid Mechanics Section
National Bureau of Standards
Washington 25, D. C.
Attn: Dr. G.B. Schubauer 1

U. S. Atomic Energy Commission
Technical Information Service
Extension, P. O. Box 62
Oak Ridge, Tennessee 1

Scientific and Technical
Information Facility
Attn: NASA Representative
P. O. Box 5700
Bethesda, Maryland 20014 1

Director
Langley Research Center
National Aeronautics and
Space Administration
Langley Field, Virginia 1

Director, Ames Research Lab.
National Aeronautics and Space
Adm. Moffett Field, Calif. 1

National Aeronautics and
Space Administration
Lewis Research Center
21000 Brookpark Road
Cleveland, Ohio 44135
Attn: Director 1
Mr. C.H. Hauser 1

Director
Engineering Science Division
National Science Foundation
Washington, D. C. 1

Commander
Air Force Cambridge Research
Center, 230 Albany Street,
Cambridge 39, Mass.
Attn: Geophysical Research
Library 1

Air Force Office of Scientific
Research, Mechanics Division,
Washington 25, D. C. 1

Aeronautical Library
National Research Council
Montreal Road
Ottawa 7, Canada 1

Engineering Societies Library
345 East 47th Street
New York 17, New York 1

Society of Naval Architects and
Marine Engineers
74 Trinity Place
New York 6, New York 1

Webb Institute of Naval Arch.
Glen Cove, L.I., New York
Attn: Prof. E.V. Lewis 1
Technical Library 1

The John Hopkins University
Baltimore 18, Maryland
Attn: Prof. S. Corrsin 1
Prof. O. M. Phillips 1
Prof. F. H. Clauser 1

Director
Applied Physics Laboratory
The John Hopkins University
8621 Georgia Avenue
Silver Spring, Maryland 1

New York State University
Maritime College
Engineering Department
Fort Schuyler, New York
Attn: Prof. J. J. Foody 1

California Institute of Tech.
Pasadena 4, California
Attn: Hydrodynamics Lab.
Prof. T. Y. Wu 1
Prof. A. Ellis 1
Prof. A. Costa 1
Prof. M. Plesset 1

University of California
Berkeley 4, California
Attn: Dept. of Engineering
Prof. H.A. Schade 1
Prof. J. Johnson 1
Prof. J.V. Wehausen 1
Prof. E.V. Laitone 1
Prof. P. Lieber 1
Prof. M. Holt 1

University of California
Los Angeles, California
Attn: Prof. R.W. Leonard 1
Prof. A. Powell 1

Director
Scripps Inst. of Oceanography
University of California
La Jolla, California 1

Iowa Institute of Hydraulic Research
State University of Iowa
Iowa City, Iowa
Attn: Prof. H. Rouse 1
Prof. L. Landweber 1
Prof. P.G. Hubbard 1

Harvard University
Cambridge 38, Mass.
Attn: Prof. G. Birkhoff 1
Prof. S. Goldstein 1

University of Michigan
Ann Arbor, Michigan
Attn: Engr. Research Inst. 1

Director
Ordnance Res. Laboratory
Penn. State University
University Park, Penn.
Attn: Dr. G.F. Wislicenus 1

Director
St. Anthony Falls Hydraulic Lab.
University of Minnesota
Minneapolis 14, Minnesota
Attn: Mr. J.N. Wetzel 1
Prof. B. Silberman 1
Prof. L.G. Straub 1

Mass. Inst. of Technology
Cambridge 39, Massachusetts
Attn: Prof. P. Mandel 1
Prof. M.A. Abkowitz 1

Institute for Fluid Mechanics
and Applied Mathematics
University of Maryland
College Park, Maryland
Attn: Prof. J.M. Burgers 1

Cornell Aeronautical Laboratory
Buffalo 21, New York
Attn: Mr. W.F. Milliken, Jr. 1

Brown University
Providence 12, Rhode Island
Attn: Dr. R. E. Meyer 1
Dr. W. H. Reid 1
Prof. Fred Bisshopp 1

Stevens Institute of Technology
Davidson Laboratory
Hoboken, New Jersey
Attn: Mr. D. Savitsky 1
Mr. J P. Breslin 1
Dr. D. N. Hu 1
Dr. S. J. Lukasik 1

Director
Woods Hole Oceanographic Inst.
Woods Hole, Massachusetts 1

Director
Alden Hydraulic Laboratory
Worcester Polytechnic Institute
Worcester, Massachusetts 1

Stanford University
Stanford, California
Attn: Dr. Byrne Perry
(Dept. of Civil Engr.) 1
Prof. E. Y. Hsu
(Dept. of Civil Engr.) 1
Dr. S. Kline
(Dept. of Mech. Engr.) 1

Dr. E.R.G. Eckert
Mechanical Engr. Department
University of Minnesota
Minneapolis, Minnesota 55455 1

Department of Theoretical and
Applied Mechanics
College of Engineering
University of Illinois
Urbana, Illinois
Attn: Dr. J.M. Robertson 1

Department of Mathematics
Rensselaer Polytechnic Institute
Troy, New York
Attn: Prof. R.C. DiPrima 1

Southwest Research Institute
8500 Culebra Road
San Antonio 6, Texas
Attn: Dr. H. N. Abramson 1

Department of Aeronautical
Engr. Univ. of Colorado
Boulder, Colorado
Attn: Prof. M. S. Uberoi 1

Courant Institute
New York University
New York, New York
Attn: Prof. P. Garabedian 1

Institut fur Schiffbau der
Universitat Hamburg
Lammersieth 90
Hamburg 33, Germany
Attn: Prof. O. Grim 1
Prof. K. Wieghardt 1

Max-Planck Institut fur
Stromungsforschung
Bottingerstrasse 6-8
Gottingen, Germany
Attn: Dr. H. Reichardt, Dir. 1

Versuchsanstalt fur Wasserbau
und Schiffbau
Gartenufer (Schleuseninsel)
1 Berlin 12, Germany
Attn: Prof.Dr.Ing. S. Schuster 1

Netherlands Ship Model Basin
Wageningen, The Netherlands
Attn: Ir.R. Wereldsma 1
Dr. J. B. Van Manen 1

Mitsubishi Shipbuilding and
Engineering Company
Nagasaki, Japan
Attn: Dr. K. Taniguchi 1

Mr. W.R. Wiberg, Chief
Marine Performance Staff
The Boeing Company
Aero-Space Division
P. O. Box 3707
Seattle 24, Washington 1

Mr. William P. Carl
Grumman Aircraft Corporation
Bethpage, L.I., New York 1

Grumman Aircraft Corporation
Bethpage, L.I., New York
Attn: Engineering Library
Plant 5 1
Mr. Leo Geyer 1

Dr. A. Ritter
Therm Advanced Research Div.
Therm, Incorporated
Ithaca, New York 1

HYDRONAUTICS, Incorporated
Pindell School Road,
Howard County, Laurel, Md.
Attn: Mr. P. Eisenberg
(President) 1
Mr. M. P. Tulin
(Vice President) 1

Dr. J. Kotik
Technical Research Group, Inc.
Route 110
Melville, New York 1

AiResearch Manufacturing Co.
9851-9951 Sepulveda Boulevard
Los Angeles 45, California
Attn: Blaine R. Parkin 1

Hydrodynamics Laboratory
Convair
San Diego 12, California
Attn: Mr. H. E. Brooke 1
Mr. R. H. Oversmith 1

Baker Manufacturing Company
Evansville, Wisconsin 1

Gibbs and Cox, Inc.
21 West Street
New York 16, New York 1

Electric Boat Division
General Dynamics Corporation
Groton, Connecticut
Attn. Mr. R. McCandliss 1

ITT Research Institute
10 W. 35th Street
Chicago 16, Illinois 1

Missile Development Division
North American Aviation, Inc.
Downey, California
Attn: Dr. E.R. Van Driest 1

National Physical Laboratory
Teddington, Middlesex, England
Attn: Head, Aerodynamics Div.
Mr. A. Silverleaf 1

Aerojet General Corporation
6352 N. Irwindale Avenue
Azusa, California
Attn: Mr. C. A. Gongwer 1

Astropower, Inc.
2121 Paularino Avenue
Newport Beach, California
Attn: R. D. Bowerman 1

Oceanics, Incorporated
Technical Industrial Park
Plainview, L.I., New York
Attn: Dr. Paul Kaplan 1

Director, Special Projects Office
Department of the Navy
Washington 25, D. C.
Attn: Code SP-001 1

National Academy of Sciences
National Research Council
Committee on Undersea Warfare
2101 Constitution Avenue
Washington 25, D. C. 1

Dr. Harvey Brooks
School of Applied Sciences
Harvard University
Cambridge, Massachusetts 1

Professor Holl
Ordnance Research Laboratory
State College, Pennsylvania 1

Ship Research Institute
Ministry of Transportation
700 Shinkawa, Mitaka
Tokyo, Japan 1

Professor F. Hammitt
College of Engineering
Nuclear Engr. Department
University of Michigan
Ann Arbor, Michigan 1

Oak Ridge National Laboratory
Post Office Box Y
Oak Ridge, Tennessee
Attn: Mr. A. Grindell 1

Scientific and Technology Division, Library of Congress
Washington, D. C. 20540 1

Mr. Jacques Dodu
Maitre de Conferences a la Faculte des Sciences
Laboratoires de Mechanique des Fluides
44-46, Avenue Felix-Viallett
Grenoble (Isere), France 1

Defense Metals Information Center, Battelle Memorial Institute, 505 King Avenue,
Columbus 1, Ohio 1

Mr. James P. Couch (500-309)
National Aeronautics and Space
Administration
21000 Brookpark Road
Cleveland, Ohio 44135 1

Documents/Reports Section
Scripps Library
Scripps Institution of
Oceanography
La Jolla, California 92037 1

Manager, Oceanics Division
Lockheed-California Co.
3380 North Harbor Drive
San Diego, California 92101 1

Professor Owen L. White
Civil Engineering Department
University of Waterloo
Waterloo, Ontario, Canada 1

Mrs. Eileen Cubberley
Government Publications Assistant
The Library, University of Waterloo
Waterloo, Ontario, Canada 1

The Principal
College of Engineering
Guindy, Madras-25
India 1

UNCLASSIFIED

Security Classification

DOCUMENT CONTROL DATA - R&D

(Security classification of title, body of abstract and indexing annotation must be entered when the overall report is classified)

1. ORIGINATING ACTIVITY *(Corporate author)*
HYDRONAUTICS, Incorporated
Pindell School Road, Howard County,
Laurel, Maryland

2a. REPORT SECURITY CLASSIFICATION
Unclassified

2b. GROUP

3. REPORT TITLE

ON MODELING CAVITATION DAMAGE

4. DESCRIPTIVE NOTES *(Type of report and inclusive dates)*
Technical Report

5. AUTHOR(S) *(Last name, first name, initial)*

Thiruvengadam, A.

6. REPORT DATE	7a. TOTAL NO. OF PAGES	7b. NO. OF REFS
August 1966	52	29

8a. CONTRACT OR GRANT NO.	9a. ORIGINATOR'S REPORT NUMBER(S)
Nonr 3755(00)(FBM) NR 062-293	Technical Report 233-10
b. PROJECT NO.	
c.	9b. OTHER REPORT NO(S) *(Any other numbers that may be assigned this report)*
d.	

10. AVAILABILITY/LIMITATION NOTICES

Qualified requesters may obtain copies of this report from DDC.

11. SUPPLEMENTARY NOTES	12. SPONSORING MILITARY ACTIVITY
	Office of Naval Research Department of the Navy

13. ABSTRACT

The intensity of bubble collapse is defined as the power transmitted per unit surface area of the bubble when the collapse pressure is a maximum and is given by the square of the collapse pressure divided by the acoustic impedence of the liquid. The efficiency of damage is defined as the ratio of the intensity of erosion of the material to the intensity of bubble collapse. Quantitative analysis is made to show how this efficiency would be affected by various physical effects such as inertia, damping of gas and vapor inside the bubble, heat transfer, compressibility, surface tension and viscosity. Experimental results with vibratory apparatus show that the efficiency of damage is primarily controlled by the damping of non-condensible gases and vapor. At higher temperature viscosity also seems to be important. Within the range of experiments, surface tension of the liquids tested seems to be unimportant. The group of non-dimensional numbers derived from the above analysis as used to formulate a modeling technique to predict the rate of depth of erosion in actual operating hydrodynamic systems.

DD FORM 1 JAN 64 1473

D23558

UNCLASSIFIED

Security Classification

14. KEY WORDS	LINK A		LINK B		LINK C	
	ROLE	WT	ROLE	WT	ROLE	WT
Cavitation damage						
Model tests						
Non-dimensional numbers						
Scaling laws						
Physical effects						
Inertia, Damping, heat transfer						
Compressibility, viscosity, surface tension						
Intensity of bubble collapse						
Efficiency of damage						

INSTRUCTIONS

1. ORIGINATING ACTIVITY: Enter the name and address of the contractor, subcontractor, grantee, Department of Defense activity or other organization *(corporate author)* issuing the report.

2*a*. REPORT SECURITY CLASSIFICATION: Enter the overall security classification of the report. Indicate whether "Restricted Data" is included. Marking is to be in accordance with appropriate security regulations.

2*b*. GROUP: Automatic downgrading is specified in DoD Directive 5200.10 and Armed Forces Industrial Manual. Enter the group number. Also, when applicable, show that optional markings have been used for Group 3 and Group 4 as authorized.

3. REPORT TITLE: Enter the complete report title in all capital letters. Titles in all cases should be unclassified. If a meaningful title cannot be selected without classification, show title classification in all capitals in parenthesis immediately following the title.

4. DESCRIPTIVE NOTES: If appropriate, enter the type of report, e.g., interim, progress, summary, annual, or final. Give the inclusive dates when a specific reporting period is covered.

5. AUTHOR(S): Enter the name(s) of author(s) as shown on or in the report. Enter last name, first name, middle initial. If military, show rank and branch of service. The name of the principal author is an absolute minimum requirement.

6. REPORT DATE: Enter the date of the report as day, month, year; or month, year. If more than one date appears on the report, use date of publication.

7*a*. TOTAL NUMBER OF PAGES: The total page count should follow normal pagination procedures, i.e., enter the number of pages containing information.

7*b*. NUMBER OF REFERENCES: Enter the total number of references cited in the report.

8*a*. CONTRACT OR GRANT NUMBER: If appropriate, enter the applicable number of the contract or grant under which the report was written.

8*b*, 8*c*, & 8*d*. PROJECT NUMBER: Enter the appropriate military department identification, such as project number, subproject number, system numbers, task number, etc.

9*a*. ORIGINATOR'S REPORT NUMBER(S): Enter the official report number by which the document will be identified and controlled by the originating activity. This number must be unique to this report.

9*b*. OTHER REPORT NUMBER(S): If the report has been assigned any other report numbers *(either by the originator or by the sponsor)*, also enter this number(s).

10. AVAILABILITY/LIMITATION NOTICES: Enter any limitations on further dissemination of the report, other than those imposed by security classification, using standard statements such as:

(1) "Qualified requesters may obtain copies of this report from DDC."

(2) "Foreign announcement and dissemination of this report by DDC is not authorized."

(3) "U. S. Government agencies may obtain copies of this report directly from DDC. Other qualified DDC users shall request through _____."

(4) "U. S. military agencies may obtain copies of this report directly from DDC. Other qualified users shall request through _____."

(5) "All distribution of this report is controlled. Qualified DDC users shall request through _____."

If the report has been furnished to the Office of Technical Services, Department of Commerce, for sale to the public, indicate this fact and enter the price, if known.

11. SUPPLEMENTARY NOTES: Use for additional explanatory notes.

12. SPONSORING MILITARY ACTIVITY: Enter the name of the departmental project office or laboratory sponsoring *(paying for)* the research and development. Include address.

13. ABSTRACT: Enter an abstract giving a brief and factual summary of the document indicative of the report, even though it may also appear elsewhere in the body of the technical report. If additional space is required, a continuation sheet shall be attached.

It is highly desirable that the abstract of classified reports be unclassified. Each paragraph of the abstract shall end with an indication of the military security classification of the information in the paragraph, represented as *(TS), (S), (C), or (U)*.

There is no limitation on the length of the abstract. However, the suggested length is from 150 to 225 words.

14. KEY WORDS: Key words are technically meaningful terms or short phrases that characterize a report and may be used as index entries for cataloging the report. Key words must be selected so that no security classification is required. Identifiers, such as equipment model designation, trade name, military project code name, geographic location, may be used as key words but will be followed by an indication of technical context. The assignment of links, roles, and weights is optional.